Structural control and tectono-sedimentary evolution of the Gulf of Cadiz, SW Iberia since the late Miocene: Implications for contourite depositional system

Débora Duarte [a,b,*], Cristina Roque [c,d], Zhi Lin Ng [a], F. Javier Hernández-Molina [a], Vitor Hugo Magalhães [b,d], Sónia Silva [e], Estefanía Llave [f]

[a] Dept. Earth Sciences, Royal Holloway Univ, London, Egham, Surrey TW20 0EX, UK
[b] Divisão de Geologia e Georrecursos Marinhos, Instituto Português do Mar e da Atmosfera – IPMA, 1749-077 Lisbon, Portugal
[c] Estrutura para a Missão de Extensão da Plataforma Continental, EMEPC, Paço d'Arcos, Portugal
[d] Instituto D. Luiz – IDL, Universidade de Lisboa, Lisbon, Portugal
[e] Centro de Ciências do Mar – CCMAR, Universidade do Algarve, Faro, Portugal
[f] Instituto Geológico y Minero de España – IGME, Madrid, Spain

ARTICLE INFO

ABSTRACT

The Gulf of Cadiz Contourite Depositional System (GCCS) developed due to the interaction of the Mediterranean Outflow Water (MOW) with the middle continental slope of the SW Iberian continental margin. The GCCS evolved in a complex tectonic setting within the foreland of the Betic Orogeny and near the Nubia-Eurasia plate boundary. This study used tectonostratigraphic analysis of an extensive 2D multichannel seismic reflection dataset to investigate how inherited basin configuration and tectonic activity controlled sedimentary stacking pattern and evolution of the GCCS. Three regional tectonostratigraphic units (U1-U3) were recognised in the margin. The younger seismic unit U3 corresponds to the Miocene-Quaternary foreland basin system where the contourite system is generated. Seismic analysis also detected the dextral strike-slip Gil Eanes Fault Zone (described herein for the first time), the Cadiz Fault, the Albufeira-Guadalquivir-Doñana Basement High and several diapiric structures. Integrated analysis of seismic profiles showing these tectonic structures with thickness and earthquake distribution maps suggest four tectono-sedimentary domains. The distinct characteristics shown by contourite features in the different domains, depends at broad-scale on the tectonic-control of the accommodation space (i.e., subsidence or uplift) and at local-scale on the presence of structural highs and fault-related depressions. Both influence bottom-current circulation and thus the evolution of the contourite deposits through the late Miocene and Quaternary. Three main stages have been recognised in the Gulf of Cadiz evolution: 1) the region was the western continuation of the Betic Corridor until the final re-opening of the Strait of Gibraltar (8–5.3 Ma). In this stage there is a predominance of turbidites or hemipelagic deposits, dependant on tectonic activity; 2) with the final re-opening of the Mediterranean-Atlantic connection there is the onset of the Pliocene-Quaternary contourite depositional system (5.3–2.0 Ma). Short-term changes in sedimentation during this stage, from contourite to turbidite deposits, indicate periods of increased tectonic activity; and 3) after the onset of the transpressive tectonic regime in the area (from 2.0 Ma), sedimentation became more homogeneous suggesting stable conditions (decrease of tectonic activity) with dominant contourite deposition. This work highlights the remarkable influence of structural features and tectonic events in controlling the seafloor relief and in turn in influenced the local oceanic circulation processes that controlling the morphology and sedimentary evolution of contourite systems.

* Corresponding author at: Dept. Earth Sciences, Royal Holloway Univ, London, Egham, Surrey TW20 0EX, UK.
E-mail address: Debora.Duarte.2017@live.rhul.ac.uk (D. Duarte).

1. Introduction

The basin-scale development and architecture of deep-water sedimentary systems depends on the interaction of tectonics, climate and sea-level changes (Mack, 1978; Artoni et al., 2007; Leeder, 2011). Tectonic activity can influence climate and eustatic changes, but interaction among these phenomena remains poorly understood (Artoni et al., 2007 and references therein). Tectonics can influence the evolution of deep-water sedimentary systems (Clark and Cartwright, 2009; Leeder, 2011) at regional scales by regulating lithospheric subsidence and uplift (e.g., orogenesis and subduction accretion) and at local scales through deformation by individual structures (e.g., folds and faults). Both condition seafloor topography by creating geomorphologic highs or depressions, which diverts or favour down- and along-slope sedimentary processes (Clark and Cartwright, 2009; Hernández-Molina et al., 2016). The majority of studies addressing these topics have focused on tectonic and structural control of down-slope processes such as landslides (Carlini et al., 2016; León et al., 2020; Silva et al., 2020; Watson et al., 2020) and turbidity currents (Clark and Cartwright, 2009, 2011; Ghielmi et al., 2013; Tinterri and Tagliaferri, 2015). A relatively limited number of studies have addressed the role of tectonics in the development and evolution of contourite depositional systems (García et al., 2009; Capella et al., 2017; Bailey et al., 2021; Liu et al., 2021; Tilley et al., 2021).

The Gulf of Cadiz (Fig. 1a, b) is an excellent setting for investigating the evolution of deep-water depositional systems in the presence of long term to ongoing tectonic activity (Rosas et al., 2009; Rogerson et al., 2012; Duarte et al., 2011, 2013; Hernández-Molina et al., 2003, 2006; Hernández-Molina et al., 2014a, 2014b; Hernández-Molina et al., 2016; Llave et al., 2007, 2011; Sánchez-Leal et al., 2017). This setting has favoured the development of an extensive contourite depositional system along the northern continental slope of the Gulf of Cadiz (Llave et al., 2007, 2011, 2019; Roque et al., 2012; Hernández-Molina et al., 2003, 2016 and references therein). Referred to as the Gulf of Cadiz Contourite Depositional System (GCCS), this system formed due to the circulation of the Mediterranean Outflow Water (MOW; Fig. 1b) into the Atlantic through the Strait of Gibraltar following the reestablishment of the Mediterranean-Atlantic connection after the Messinian Salinity Crisis at 5.3 Ma (Flecker et al., 2015). Salt and mud diapirism have also affected the system (Fernández-Puga et al., 2007; Medialdea et al., 2009; Matias et al., 2011; García et al., 2020).

Although studies conducted thus far have addressed tectonic and diapiric activity in the GCCS (Nelson et al., 1999; Llave et al., 2001; García et al., 2009; Roque et al., 2012; Hernández-Molina et al., 2003; Hernández-Molina et al., 2014a, 2014b; Hernández-Molina et al., 2016; García et al., 2020), these have focused on small and specific areas of the system and thus lacked a basin-scale perspective. They also present only general structural or spatial analysis and are restricted to the Late Quaternary time frame. Uncertainties persist regarding the role of tectonics and diapirism in the development and evolution of the Gulf of Cadiz deep-water sedimentary systems (i.e., contourite and turbidite systems) especially at regional scales since the late Miocene.

The present research offers a detailed tectonostratigraphic and structural analysis of late Miocene through Quaternary deep-water sedimentary systems in the Gulf of Cadiz based on an extensive 2D seismic dataset (Fig. 1c). The research specifically sought to i) determine structural influences on the development and evolution of the deep-water sedimentary systems at basin-scale, with particular emphasis on the GCCS, ii) present detailed structural and seismotectonic analysis and mapping of the study areas including novel features such as the Gil Eanes Fault Zone and iii) develop a model of tectono-sedimentary evolution for the deep-water depositional system since the late Miocene.

2. Regional setting

2.1. Geological and oceanographic setting

The Gulf of Cadiz encompasses the region west of the Strait of Gibraltar between the SW Iberian and NW African margins (Fig. 1a, b). It formed during the Triassic-Lower Cretaceous opening of the North Atlantic and Western Tethys (Neo-Tethys) oceans (Maldonado et al., 1999; Ramos et al., 2016). Extension was accommodated by *E*-W to ENE-WSW normal faults and NW-SE to NNW-SSE transfer zones (Terrinha et al., 2013; Terrinha et al., 2019a; Ramos et al., 2020). The transfer fault system consists of the N-S Portimão Fault (Terrinha et al., 2003; Fig. 1b) and the NW-SE São Marcos-Quarteira Fault Zone (Cabral et al., 2017, 2019; Fig. 1b) which parse the Algarve Basin into distinct blocks.

Since the Late Cretaceous, Africa-Eurasia plate convergence has determined the structural evolution of the Gulf of Cadiz (Vergés and Fernàndez, 2012; Terrinha et al., 2019b). Collision between these two plates resulted in the development of the Betic-Rif orogenic system, also known as the Gibraltar Arc, which comprises the Alboran back-arc and the Guadalquivir and Rharb foreland basins (Vergés and Fernàndez, 2012). Westward migration of the Betic-Rif domain led to the formation of a massive chaotic body of deformed late Mesozoic-Cenozoic strata around the Gulf of Cadiz region in the late Tortonian (~8 Ma; Maldonado et al., 1999; Medialdea et al., 2004; Iribarren et al., 2009; Terrinha et al., 2019b). The chaotic body includes the Gulf of Cadiz Accretionary Wedge (GCAW) and related gravitational allochthonous units (Medialdea et al., 2004; Iribarren et al., 2007). The GCAW deposited over remnant Tethys oceanic crust, and its development reflects eastward dipping subduction of the oceanic lithospheric slab beneath the Gibraltar arc (Gutscher et al., 2002; Terrinha et al., 2019b). The basin also records late Miocene-Pliocene closure of the Mediterranean–Atlantic marine connections due to continuous continental collision along the Betic-Rif Arc and isostatic rebound related to slab roll back and slab-dragging (Duggen et al., 2003; Vergés and Fernàndez, 2012; Spakman et al., 2018). These events led to the Messinian Salinity Crisis (5.97–5.33 Ma; Flecker et al., 2015).

Presently, the SW Iberian margin experiences transpression and NW–SE to WNW–ESE compression (Terrinha et al., 2009; Zitellini et al., 2009; Cunha et al., 2012) at a rate of ca. 4.5–6.0 mm/yr (Cunha et al., 2012; Vergés and Fernàndez, 2012). The present-day kinematics commenced no later than 1.8 Ma with the latest Iberian-African plate boundary reorganization (Rosas et al., 2009). The plate boundary is diffuse, with evidence of strain partitioning along WNW–ESE dextral strike-slip faults (the SWIM faults) and NE–SW thrust faults (Zitellini et al., 2009; Terrinha et al., 2019b). Seismicity along the northern margin of the Gulf of Cadiz consists of frequent low to intermediate magnitude events ($M_w < 5.0$, Fig. 1b). The region has experienced large historical and instrumental earthquakes such as the 1755 Lisbon Earthquake and Tsunami ($M_w \geq 8.5$, Baptista et al., 1998; Johnston, 1996), the 1969 Horseshoe Earthquake (M_w 7.0–8.0, Fukao, 1973), and more recently, the 2007 Horseshoe Fault Earthquake ($M_w = 6.0$, Stich et al., 2007).

The Mediterranean Outflow Water (MOW) exits the Mediterranean Sea through the Strait of Gibraltar and flows as an intermediate contour current along the SW Iberian Margin (Fig. 1b) between water depths of 500 and 1400 m (Sánchez-Leal et al., 2017). After exiting through the Strait of Gibraltar, the MOW spreads westward along the SW Iberian middle slope, where it has built up the GCCS (Fig. 1b) throughout the Pliocene-Quaternary within the Algarve, Doñana, Sanlucar and Cadiz basins (Llave et al., 2007, 2011, 2019; Roque et al., 2012; Hernández-Molina et al., 2003, 2016).

Interactions with complex seafloor morphology (canyons, diapiric ridges and basement highs) cause the MOW to split into two main branches (Ambar and Howe, 1979; Serra et al., 2005; Zenk and Armi, 1990) including a less saline and warmer Mediterranean Upper Core (500–700 m) and a more saline and colder Mediterranean Lower Core
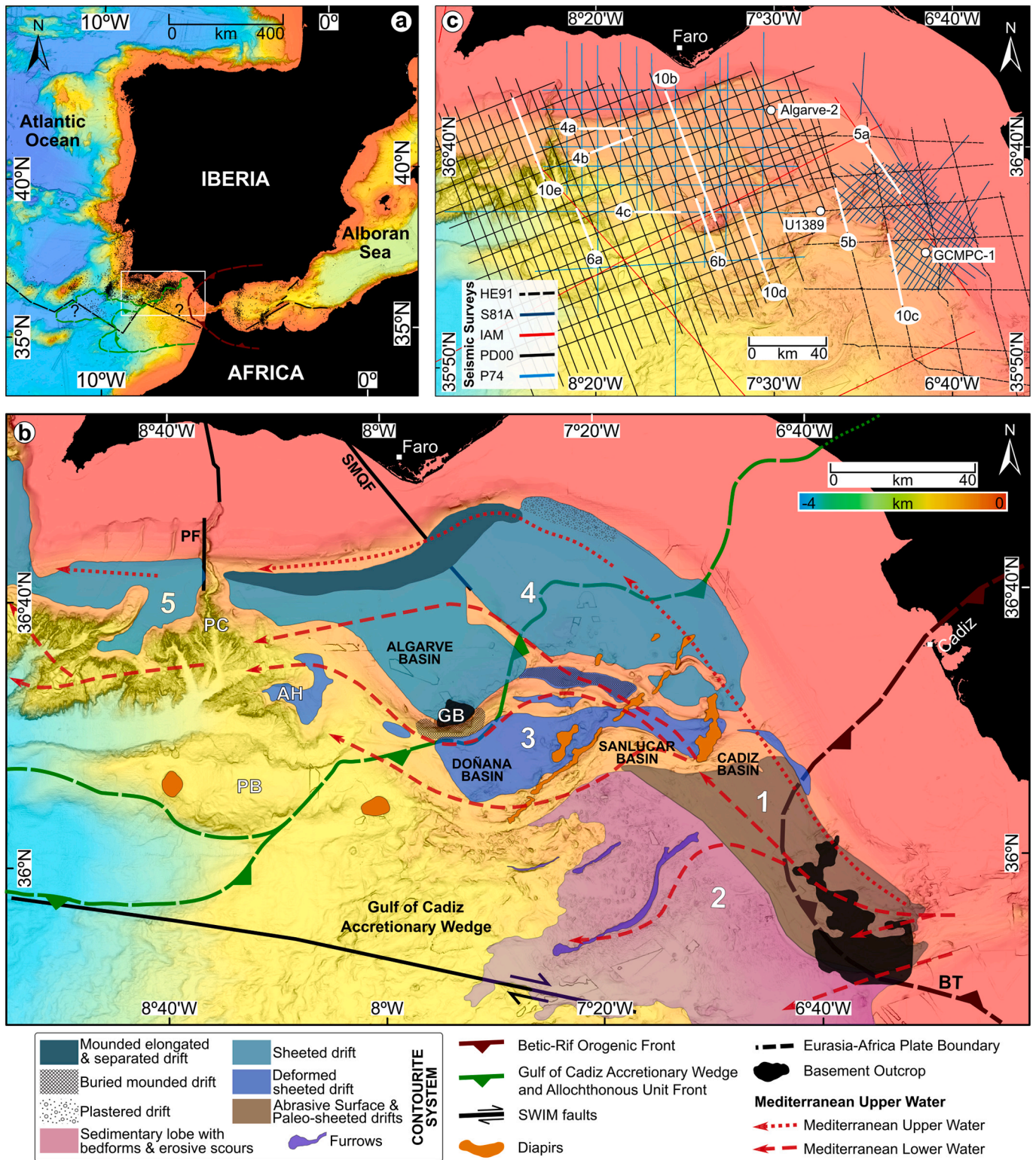
Fig. 1. Geographic location of the study area (white rectangle) and a) regional setting with the main tectonic structures. Black circles show earthquake locations (Further details in Fig. 8 and Fig. S1 and S2); b) Detailed map of the study area showing the main structural features, the Mediterranean Outflow Water pathway and the Gulf of Cadiz Contourite System morphosedimentary sectors (1 to 5). These are: 1) proximal scour and ribbons sector, 2) overflow sedimentary lobe sector, 3) channels and ridges sector, 4) contourite depositional sector and 5) submarine canyons sector. GB: Guadalquivir Bank, PB: Portimão Bank, AH: Albufeira High, PF: Portimão Fault, SMQF: São Marcos-Quarteira Fault. c) Dataset used in this work. Bathymetric data come from the EMODnet Digital bathymetric database. Grid cell resolution is ~115 m (EMODnet Bathymetry Consortium, 2018).

(800–1400 m). The Lower Core further divides into three minor branches referred to as the southern, the principal and the intermediate branches.

2.2. Palaeoceanography of the MOW and contourite features

The connection between the Atlantic Ocean and the Mediterranean Sea became established in the late Miocene through several marine gateways in southern Spain (Betic Corridor), northern Morocco (Rifian

Table 1
Main seismic facies for the *U3* seismic sub-units (*U3a* to *U3g*). AB: Algarve Basin, DB: Doñana Basin, CB: Cadiz Basin. Age estimates for the seismic discontinuities were obtained from correlation with well data (Hernández-Molina et al., 2016; Ng et al., 2021b).

Seismic sub-unit	Seismic Facies		Average thickness	Seismic horizon	Age
	Shape and terminations	*Internal configuration*			
				SF	0 Ma
U3g	Regional draped geometry. Conformable with *U3f*, in basins' centre. Mostly aggradational geometries. Small, mounded to the north of the AB.	Good continuity, low to medium amplitude reflections in the AB, and stronger amplitudes in the basins on top of seismic unit *U2*.	0.13 s TWT		
				f	0.6-0.3 Ma
U3f	Regional draped geometry. Conformable in the basins' centre with *U3e*, but onlapping in the margins or diapirs. Mostly aggradational, but mounded geometries in the north of the AB.	Good lateral continuity, low to medium amplitude reflections in the AB. Stronger amplitudes in the basins on top of seismic unit *U2*.	0.12 s TWT		
				e	0.9-0.7 Ma
U3e	Regional draping geometry. Conformable to *U3d*, in the basins' centre. Mostly aggradational, but mounded geometries are observed to the north of the AB and DB.	Low amplitude reflection in the base, evolving upwards into higher amplitudes. Good lateral continuity and sub-parallel reflections.	0.09 s TWT		
				d	1.5-1.3 Ma
U3d	Regional draping geometry. Conformable to U3c in the basins' centre, but onlapping in the margins or diapirs. Mostly aggradational, but mounded geometries are observed to the north of the AB and DB.	Internal reflections show variable medium to high amplitude, good lateral continuity, parallel reflections. Semi-transparent facies also observed.	0.43 s TWT		
				c	2.3-2.0 Ma
U3c	Regional draped geometry, with infill geometry onlapping into the basins' margins. Aggradational deposits.	Semi-transparent and weak sub-parallel reflections, with increasing amplitude towards the top and good lateral continuity.	0.13 s TWT		
				b	3.2-3.0 Ma
U3b	Infill geometry onlapping into the basins' margins. Aggradational in the AB (max. 0.48 s TWT). Higher sedimentary rates in the CB (max. 1.21 s TWT).	Low to moderate amplitudes evolving upwards into high amplitude reflections, with good lateral continuity in the AB. Semi-transparent to weak amplitudes in the basins on top of seismic unit *U2*.	0.32 s TWT		
				a	6.4 Ma
U3a	Regional sheeted geometry. Mostly aggradational, but channelized facies are observed locally.	Transparent or very low amplitudes, sub-parallel reflections. High amplitude locally. Good lateral continuity in the AB, while poor continuity is observed in basins on top of *U2*.	0.16 s TWT		
				T2/T3	~20 to 8.0 Ma

AB: Algarve Basin, DB: Doñana Basin, CB: Cadiz Basin

AB: Algarve Basin, DB: Doñana Basin, CB: Cadiz Basin

Corridor) and possibly also through the Gibraltar region (Flecker et al., 2015; Krijgsman et al., 2018). Contourite features related to the circulation of the palaeo-MOW have been recognised in both the Betic and Riffian Corridors (Martín et al., 2009; Capella et al., 2017; de Weger et al., 2020, 2021). Ng et al. (2021a, 2021b) recently reported evidence for the existence of a late Miocene contourite depositional system in the Gulf of Cadiz. Turbiditic deposits have also been recognised in the Guadalquivir Basin and the Cadiz continental shelf (Riaza and Olmo, 1996; Ledesma, 2000; Mestdagh et al., 2020).

Continuous tectonic uplift of the Betic-Rif region caused closure of the Mediterranean-Atlantic marine connections and exhumation of the Betic and Rifian Corridors by the early Messinian, but exchange at shallow levels could continue across a proto-Gibraltar Strait (Capella et al., 2018; Krijgsman et al., 2018). Restricted circulation of palaeo-MOW led to the Messinian Salinity Crisis in the Mediterranean (Flecker et al., 2015) and general deposition of hemipelagites on the Atlantic side of the margin (i.e., Gulf of Cadiz; Ng et al., 2021b). Following early Pliocene re-establishment of the Mediterranean-Atlantic connection, the Gulf of Cadiz has hosted water exchange between the Mediterranean Sea and the Atlantic Ocean through the Strait of Gibraltar (Rogerson et al., 2012).

Climatic and sea-level variations have caused depth and spatial fluctuations in the MOW during the Pliocene-Quaternary (Nelson et al., 1999; Hernández-Molina et al., 2006; Voelker et al., 2006; Sierro et al., 2020). During glacial episodes, the current possessed higher density and salinity and would flow at deeper water levels (Rogerson et al., 2005; Hernández-Molina et al., 2006; Llave et al., 2006; Voelker et al., 2006). During interglacial periods, a weaker MOW split into several branches and occupied positions similar to those observed today (Fig. 1b, Rogerson et al., 2005; Llave et al., 2006).

The Pliocene and Quaternary development of the GCCS included three main stages: i) the initial drift stage (5.33–3.2 Ma) with a weak MOW and development of sheeted or mixed drifts, ii) a transitional drift stage (3.2–2.0 Ma) with MOW intensification and upslope drift migration and moat development, and iii) a drift growth stage (2.0–0 Ma) with continuous MOW enhancement and formation of large elongated mounded and sheeted drifts (Hernández-Molina et al., 2016).

3. Data and methods

3.1. Data

The data used in this study consisted of 2D seismic reflection profiles and instrumental seismicity compilations covering the entire study area. The 2D multichannel seismic reflection data came from the PDT00-PD00, P74, HE91, S81A and IAM surveys (Fig. 1c), which were provided (with a confidentiality agreement) by REPSOL, S.A. and TGS-Nopec. The Supplementary Material (Table 1) list cruise details and data acquisition parameters. The main processing steps included a pre-stack time migration and the application of a bandpass filter. The seismic dataset was calibrated with two industry wells drilled in Algarve and Cadiz Basins (Algarve-2 and GCMPC-1, respectively) and Site U1389 from IODP Expedition 339 in the Doñana Basin (Fig. 1c).

The IPMA earthquake catalogue (www.ipma.pt) covering the period 2003–2018 was used to identify relevant seismic events associated with structures identified in this study (Fig. 1b, Supplementary Material Figs. S1, S2 and Table S2). The catalogue includes 6400 events with magnitudes ranging between 0.1 and 6.1. This database was supplemented by events recorded in offshore temporary networks from TOP-OMED (Grevemeyer et al., 2016) and NEAREST projects (Geissler et al., 2010; Silva et al., 2017). Both networks provide better estimates of offshore seismic activity than those generated by permanent networks (Grevemeyer et al., 2016; Silva et al., 2017). However, only a few events occurred in the area during the time frame of interest.

The EMODnet Digital bathymetric compilation was used as a cartographic base map for this study (http://www.emodnet-bathymetry.eu).

It merges several high-resolution single and multiple beam bathymetric surveys with composite digital terrain models (EMODnet Bathymetry Consortium, 2018) at a grid cell resolution of ~115 m (pixel size of 1/16 arc minutes).

3.2. Methods

Seismic interpretation was performed using Petrel E&P software (Schlumberger) and based on a tectonostratigraphic analysis (Nikishin and Kopaevich, 2009). This consists on the identification of discontinuities that separate tectonostratigraphic seismic units, which were interpreted as being related to different tectonic episodes at basin-scale (e.g., *syn-rift, post-rift, syn-inversion*) and to main local tectonic structures (e.g., faults, structural highs, diapirs, folds). The specific stratal architectures displayed by tectonostratigraphic units reflect the tectonic process active during the time of their accumulation (e.g., rifting). The description of seismic facies follows the classic approach proposed by Mitchum et al. (1977a, 1977b, 1977c). The identified tectonostratigraphic units were correlated with seismostratigraphic frameworks from previous studies of the region (Maldonado et al., 1999; Ledesma, 2000; Llave et al., 2011; Roque et al., 2012; Hernández-Molina et al., 2016). Seismic-to-well tie points and chronostratigraphic ages of Pliocene-Quaternary regional discontinuities (Fig. 2) for the Gulf of Cadiz middle slope are thoroughly described in Hernández-Molina et al. (2016).

Surface maps (in milliseconds two-way-travel time; ms TWT) were generated for the main unconformities (*T1, T2* and *T3*). The basal surfaces of the Algarve, Doñana, Sanlucar and Cadiz basins were generated by combining two seismic horizons of different age and geologic nature (*T2* and *T3, Fig. 3*). The composite surface represents the palaeo-topography upon which the foreland basin system began to develop (after ~8 Ma). The separation between the two horizons is represented on maps as the GCAW front. A thickness map generated for the Miocene-Quaternary sequence shows the regional key depocentres of the Betic foreland. Maps also show the main tectonic and diapiric structures (Fig. 3b, c). Seismic grid characteristics (e.g., distance between lines, different resolution of seismic lines, etc.) and diapiric deformation occurring after the age of 8 Ma, may result in some local inaccuracies in the maps, which not invalidate their regional purpose.

Correlations between seismic events and tectonic structures considered both the proximity of the hypocentre to the structures and focal mechanisms showing a fault plane orientation compatible with the interpreted kinematics for the structure. The scattered nature, the high number of events and uncertainties in their precise location made correlations difficult. The GMT software (Wessel and Smith, 1998) was used to plot vertical profiles with the depth distribution of the earthquakes.

4. Results

4.1. Tectonostratigraphy

Three seismic units (*U1* to *U3*) bounded by discontinuities (*T1* to *T3*) appear along the Algarve, Doñana, Sanlucar and Cadiz Basins (Figs. 3, 4, 5, 6) and document different phases of tectonic and structural control at regional scales. Although the present study focuses on seismic unit *U3*, a brief description is also presented for the basement and seismic units *U1* and *U2*.

Basement

The basement is bound at its top by the seismic horizon *T1*, which is a high amplitude reflection with good lateral continuity (Fig. 6). The surface appears at shallower depths (<4 s TWT) as a structural high referred to as the Albufeira-Guadalquivir-Doñana High (AGDH). Internally, the basement exhibits discontinuous, high-amplitude, chaotic internal reflections bounded by normal faults.
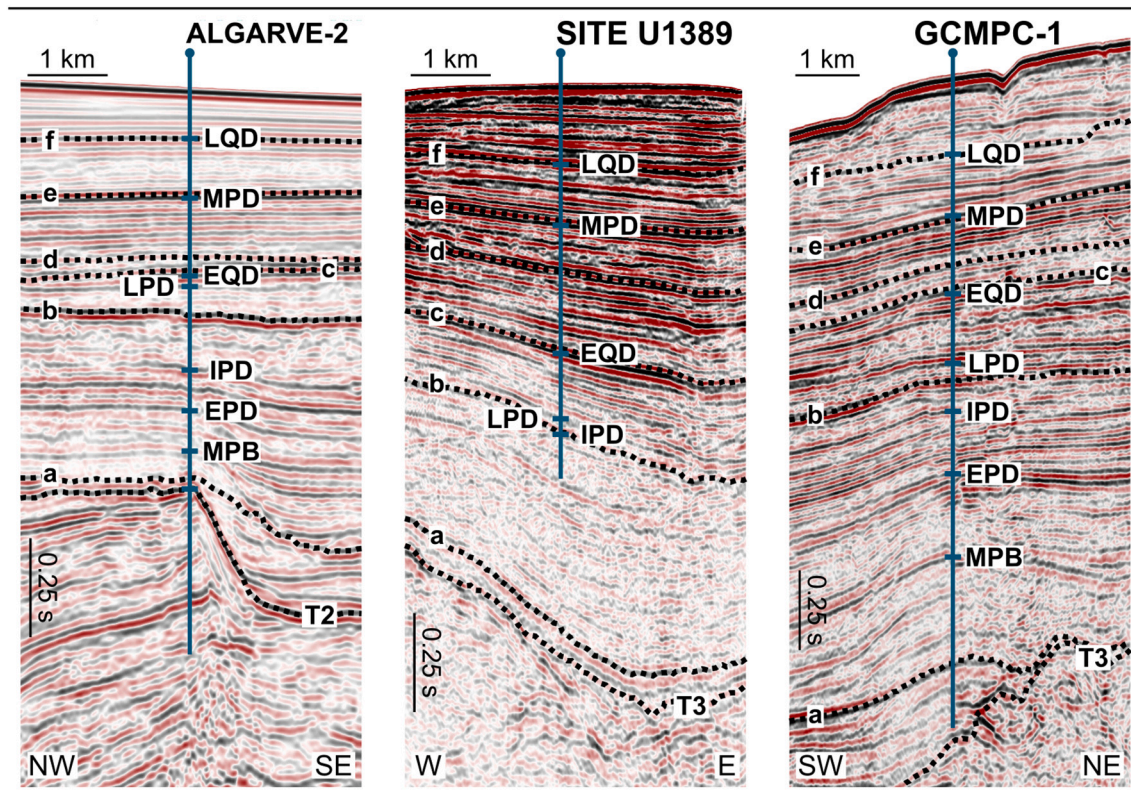
Fig. 2. Seismic sections crossing the Algarve-2, U1389 and GCMPC-1 wells. These show correlations between the recognised chronostratigraphic discontinuities and the tectonostratigraphic seismic horizons identified in the study. MPB: Miocene-Pliocene Boundary, EPD: Early Pliocene Discontinuity, IPD: Intra-Pliocene Discontinuity, LPD: Late Pliocene Discontinuity, EQD: Early Quaternary Discontinuity, MPD: Middle Pleistocene Discontinuity, LQD: Late Quaternary Discontinuity.

Seismic unit U1

The seismic unit *U1* consists of folded and faulted strata appearing as reflections varying from high amplitude and laterally continuous to more chaotic to transparent reflections with poor continuity. *U1* is bound laterally and at its base by *T1* (Figs. 3a, 4, 5, 6). The unconformity *T2* bounds the unit's top and appears as a high amplitude reflection with good lateral continuity. Locally, *T2* truncates *U1* and can appear as a more conformable reflection (paraconformity) in the centre of the basin (Figs. 3, 4, 5, 6).

Seismic unit U2

Seismic unit *U2* appears as chaotic and transparent facies and exhibits an irregular top and wedge-shaped front. It is bounded at its top by unconformity *T3*, which records an abrupt change in seismic facies and depositional style (Figs. 5, 6). *T3* appears regionally as discontinuous reflections characterised by lateral changes, with areas where the reflection is continuous and shows high amplitudes or areas where it has lower amplitudes depending on the higher or lower degree of deformation of seismic unit *U2*.

Seismic unit U3

Seismic unit *U3* exhibits a regional basin-infill geometry outlined by continuous reflections that range from transparent to high amplitude. Its basal boundary is marked by three distinct seismic horizons, *T1*, *T2* and *T3* (Fig. 3a). Internally, *U3* appears as several discontinuities in the seismic record (from *a* to *f*) characterised by continuous reflections of moderate to high amplitude that terminate as toplap or onlap features (Figs. 4, 5, 6). These bound seven sub-units (*U3a* to *U3g*) described in detail in Table 1.

4.2. Internal characteristics of seismic unit U3

Seismic unit *U3* exhibits distinctive characteristics in each basin. The Algarve Basin is an ENE-WSW elongated depocentre limited by the palaeo-continental slope to the north and by the AGDH to the south (Fig. 3). Here *U3* reaches its maximum depth of 5.25 s TWT to the SW (Fig. 3b). The thickness of *U3* varies considerably within the Algarve Basin. It reaches a maximum thickness of 1.88 s TWT in the east (dA-1, Fig. 3c and Supplementary Material Table S3) and becomes thinner (<1.35 s TWT) in the western part of the basin (Fig. 3c, Table S3). The Doñana Basin is a NE-SW elongated region between the AGDH and the Guadalquivir Diapiric Ridge consisting of various small depressions separated by diapiric highs. In this basin, seismic unit *U3* developed NE-SW elongated depocentres reaching a maximum thickness of 2.25 s TWT (dW-6 and dW-7 in Fig. 3c). The Sanlucar Basin is an NNE-SSW triangular-shaped basin widening towards the SSW and developed between the Gualdalquivir Diapiric Ridge and the Cadiz Diapiric Ridge. The Cadiz Basin developed in an NNE-SSW orientation bounded by the Cadiz Diapiric Ridge and the Betic Front Thrust (BT in Fig. 3). The basin consists of a main depression in the SSW that joins with the Sanlucar Basin (maximum depth of 3.73 s TWT), where seismic unit *U3* reaches thicknesses of 2.77 s TWT (Fig. 3c), and an NNE region, where several small, shallower rounded depressions are bound by diapirs. *U3* hosts four types of deep-water deposits. These include contourite drifts, turbidites, gravitational deposits and hemipelagic sediments. Table 2 describes these depositional features.

4.3. Tectonic structures

Three main regional tectonic structures were identified in the SW Iberian Margin separating the Miocene-Quaternary basins (Figs. 3, 4, 5, 6). These include the newly identified Gil Eanes Fault Zone and the
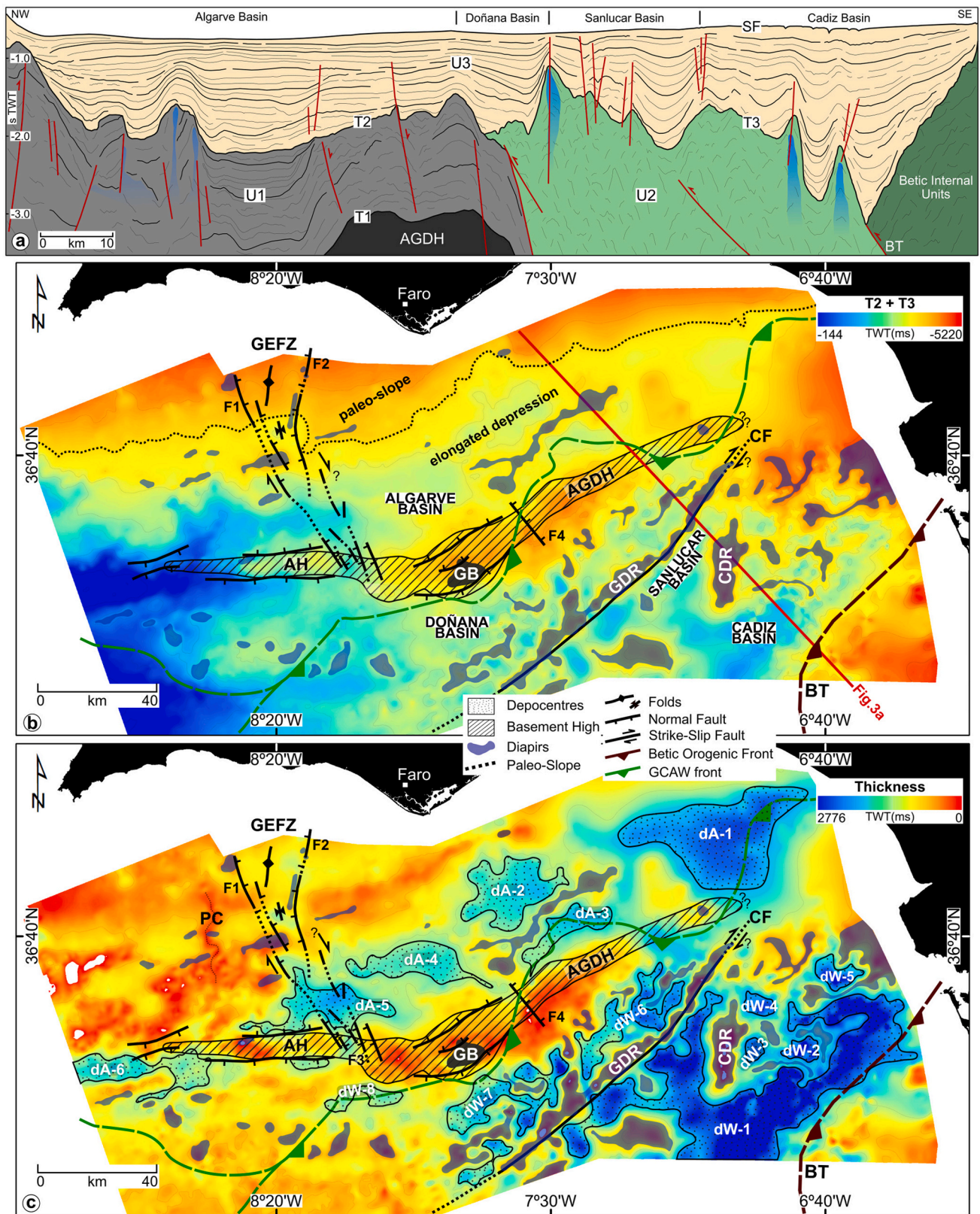
Fig. 3. a) NW-SE cross-section based on composite seismic lines including the main seismic units and basins (vertical exaggeration of 10×; approx. Location in Fig. 3b). b) Isobath map for *T2 + T3*. c) Thickness map for the Seismic Unit *U3*. dA-1 to dA-5: depocentres associated to the Algarve Basin, dW-1 to dW-8: depocentres associated to the wedge-top basins. Details of each depocentre are given in the Supplementary Material Table S3. Grey shaded areas represent diapirs. Green line shows the distal limit of the GCAW. AGDH: Albufeira-Guadalquivir-Doñana Structural High, GB: Guadalquivir Bank, AH: Albufeira High, PC: Portimão Canyon, GEFZ: Gil Eanes Fault, CF: Cadiz Fault, BT: Betic Front Thrust, GDR: Guadalquivir Diapiric Ridge, CDR: Cadiz Diapiric Ridge. (For interpretation of the references to colour in this figure legend, the reader is referred to the web version of this article.)
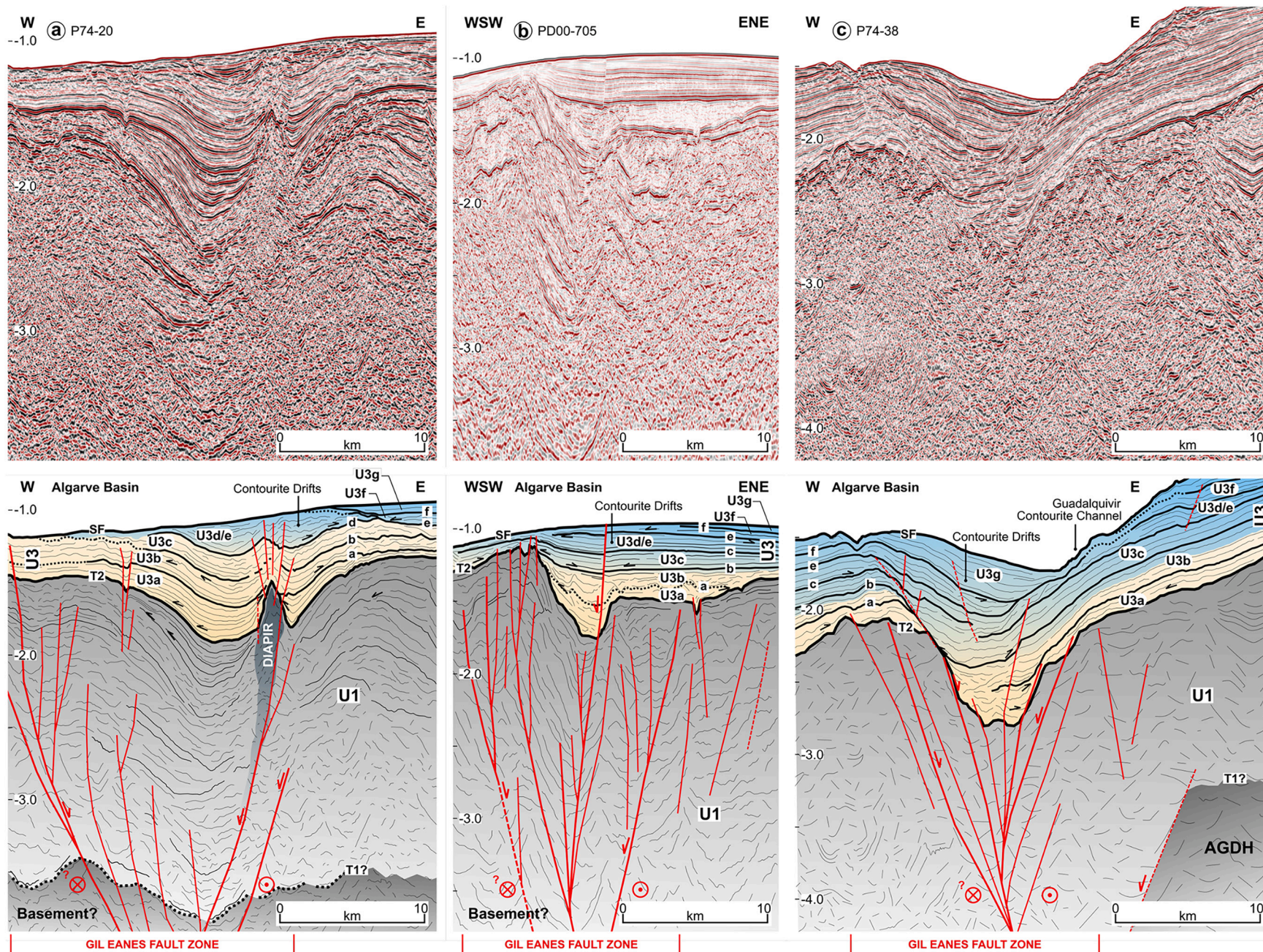
Fig. 4. Seismic sections and their interpretation crossing the Gill Eanes Fault Zone (GEFZ) with lines P74 (a), PD00–705 (b) and P74–38 (c). The main seismic units, sub-units and regional unconformities are shown. Fig. 1c gives profile location. AGDH: Albufeira-Guadalquivir-Doñana Structural High. Red symbols relate to the direction of fault movement: the circle with a point is seen on the block moving towards the observer, while the circle with a cross on the block moving away. (For interpretation of the references to colour in this figure legend, the reader is referred to the web version of this article.)
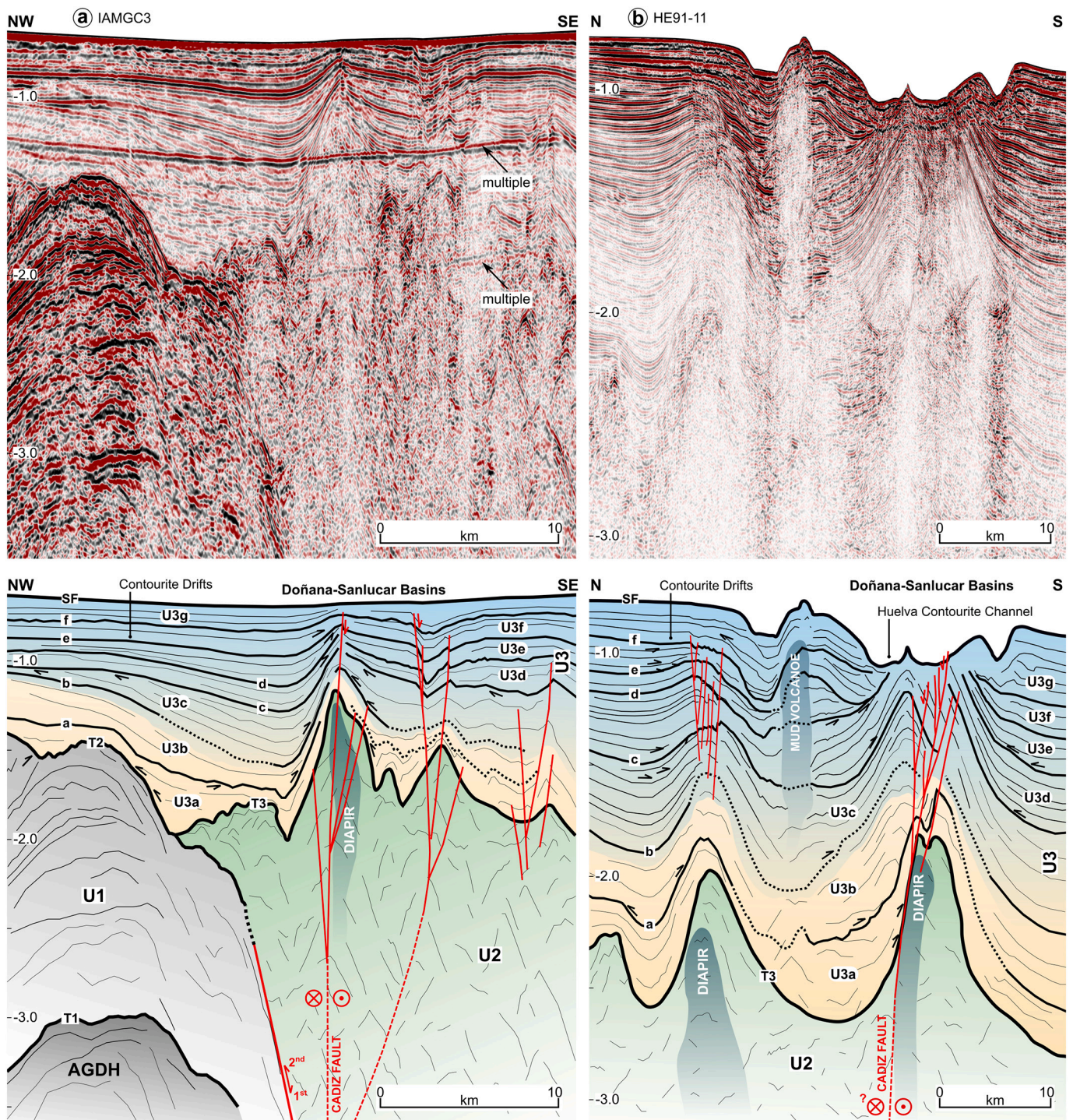
Fig. 5. Seismic sections including seismic units, sub-units, regional unconformities and interpretations for IAMGC3 (a) and HE91–11 (b) crossing the Cadiz Fault (CF). Fig. 5a shows the Albufeira-Guadalquivir-Doñana High (AGDH). Figure indicates diapiric structures and mud volcanoes associated with the GCAW (*U2*) and CF. Fig. 1c gives profile location. Red symbols relate to the direction of fault movement. (For interpretation of the references to colour in this figure legend, the reader is referred to the web version of this article.)

previously known Cadiz Fault and Albufeira-Guadalquivir-Doñana Basement High (e.g., Duarte et al., 2011; García et al., 2016). Local diapiric structures also play an important role in the basins' layout and evolution.

Gil Eanes Fault Zone (GEFZ)

The newly identified Gil Eanes Fault Zone can be observed in the Algarve Basin between the Guadalquivir Bank to the east and the Portimão Canyon and Albufeira High to the west (Fig. 3b, c). The seismic sections displayed in Fig. 4 show deformation structures associated with the Gil Eanes Fault. Several sub-parallel to parallel, partially overlapping fault planes, form a negative strike-slip flower structure rooted in a sub-vertical fault (Fig. 4a, b). Structures also show signs of dip-slip displacement, which locally affect the present-day seafloor (Fig. 4b). The northern part of the structure hosts two main faults bounding an anticlinal fold (Fig. 4a, b), which exhibits a general NNE-SSW
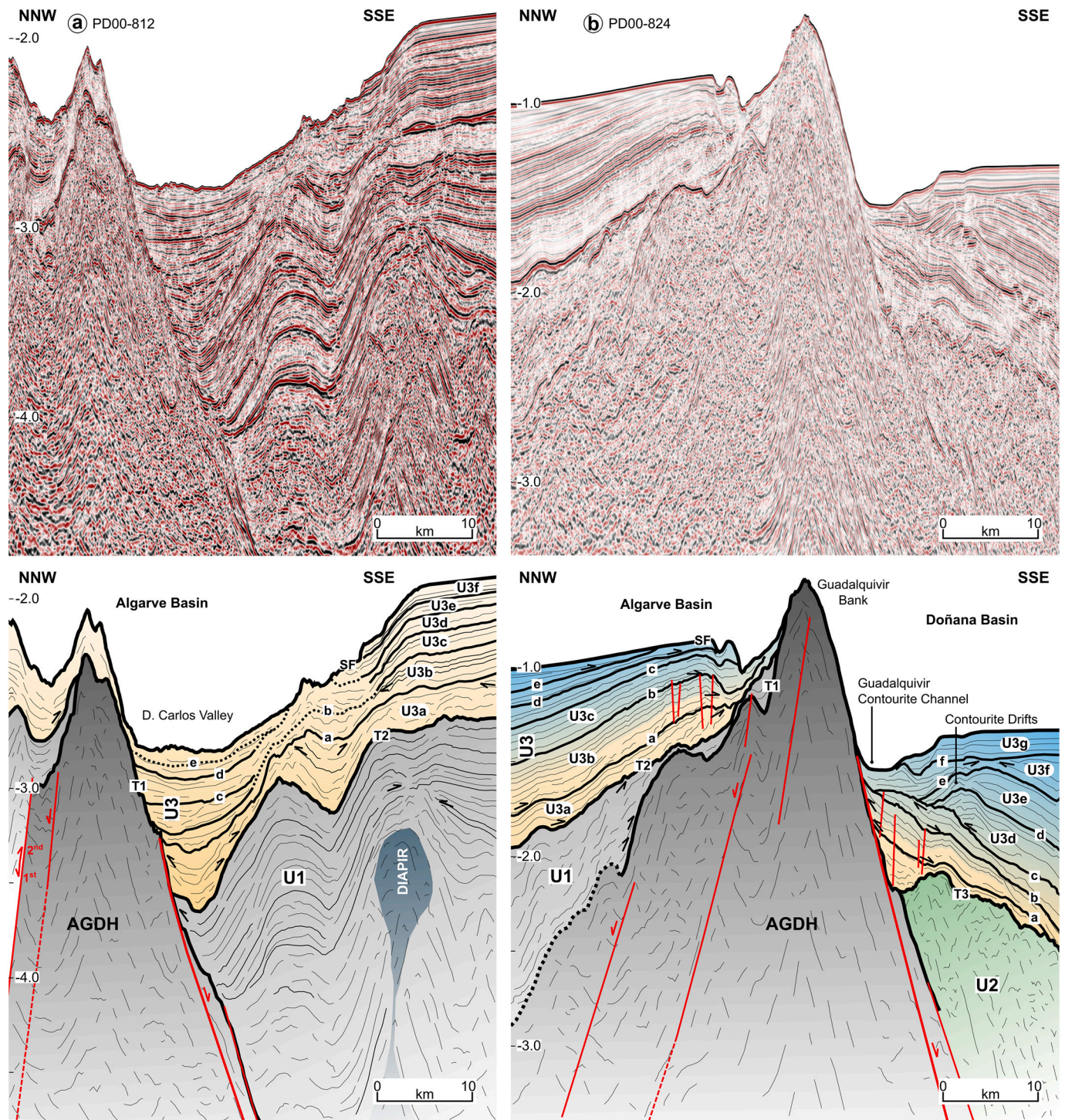
Fig. 6. Seismic sections including seismic units, sub-units and unconformities for (a) PD00–812 in the Albufeira High region and (b) PD00–824 along the Guadalquivir Bank. Figs. 1c and 7 give profile location. AGDH: Albufeira-Guadalquivir-Doñana Structural High.

orientation.

This complex structure distributed over an approximately 10 km wide (~E-W) zone extending for about 80 km in an NNW-SSE direction. The diffuse character of deformation, seismic resolution and distance between the 2D seismic grid lines make it difficult to precisely map this structure. It marks a change in margin architecture and delimits the end of the Algarve Basin's elongate depocentre region (dA-1 to dA-5; Fig. 3c). Only one depocentre appears west of the fault (dA-6, <1.35 s TWT; Fig. 3c).

Cadiz Fault (CF)

The Cadiz Fault extends for approximately 150 km and trends NE-SW to ENE-WSW starting from the Cadiz continental shelf and running south of the Guadalquivir Bank (Fig. 3b, c). It separates the Doñana (dW-6 and dW-7) and Sanlucar-Cadiz (dW-1) depocentres (Fig. 3c). The seismic profiles (Fig. 5) show a sub-vertical fault ending in a bundle of sub-parallel fault planes which deform *U3*. The Cadiz Fault was identified as a strike-slip fault based on its negative flower structure geometry. Minor vertical displacement (>0.5 s TWT) appears to locally offset the present-day seafloor (Fig. 5b). Poor seismic resolution in *U2* obscures

Table 2
Seismic sections showing the main depositional features recognised in this study along with general description and distribution.

| Deposits	Seismic Section	Characteristics	Distribution
Contourites — Mounded drifts		Mounded to sheeted, asymmetric external shapes. Low to high amplitude, sub-parallel and continuous reflections. Progradational sigmoidal configuration, with onlapping and downlapping terminations. Seawards the deposits show a more aggradational geometry.	*U3d* to *U3g* - Algarve Basin. *U3d* and *U3e* - Doñana Basin.
Contourites — Sheeted drifts		Sheet or sheet-drape external shape. Sub-horizontal deposits, with parallel to semi-parallel continuous moderate to high amplitude reflections. Evidence of erosion can be observed on the flank of the deposits.	*U3c* and *U3d* - Algarve Basin., U3c, Sanlucar and Cadiz Basins. *U3c*, *U3f* and *U3g* - Doñana Basin. *U3b*(?) to *U3f* - Cadiz Basin.
Turbidites		U-shaped convex and lateral lens external geometries. Sub-parallel, moderate to high amplitude, continuous evolving upwards into discontinuous reflections. Aggradational levees, laterally incised by erosive channels.	*U3a* and lower *U3b* - Algarve, Doñana, Sanlucar and Cadiz Basins.
Gravitational Deposits		Lenticular external geometry, with deformed internal architecture and an irregular top. Semi-continuous to discontinuous reflections changing upwards into chaotic reflections, with moderate to high amplitudes. Transparent zones can also be observed.	Mostly upper *U3b* - Algarve Basin. Local gravitational deposits could be observed throughout *U3*.
Hemipelagic/Pelagic deposits		Sheet-drape external geometry. Parallel to sub-parallel, continuous reflections, with low to high amplitudes.	*U3a* and lower *U3b* - Algarve, Doñana, Sanlucar and Cadiz Basins. *U3* - western Doñana Basin (as observed in the seismic section).

deeper parts of this structure.

Albufeira-Guadalquivir-Doñana High (AGDH)

The AGDH is an elongated morpho-structural basement high that extends for about 200 km (Fig. 3b, c). In seismic data it appears as high amplitude triangular features with chaotic internal facies bounded by normal faults (Fig. 6).

The *T1* isobath map indicates the AGDH consists of three sectors from west to east (Fig. 7). Sector 1 (Albufeira High region) trends in an E-W direction. Sector 2 corresponds to the Guadalquivir Bank. Sector 3 (east of the Guadalquivir Bank) trends in an ENE-WSW direction. Sectors 1 and 2 are divided by the Gil Eanes Fault. A sharp decrease in depth (from 2 s to 2.75 s TWT) occurs between sectors 2 and 3 indicating the presence of a NW-SE normal fault (F4 in Fig. 7).

In sectors 1 and 3, the AGDH reaches depths between 3 and 2.5 s TWT. It is overlain by thinner sedimentary cover (seismic unit *U3*) in
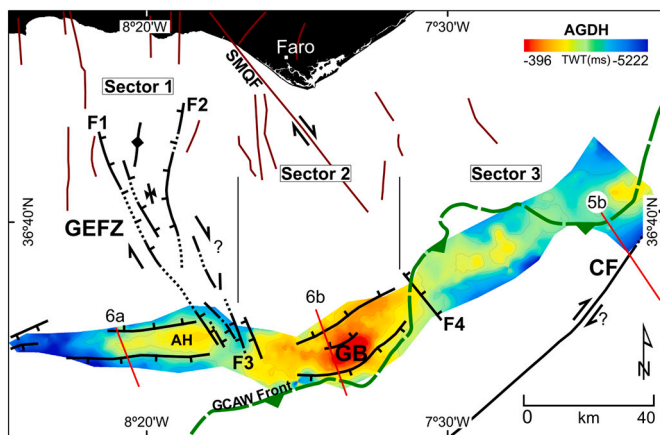
Fig. 7. Isobath map for the Albufeira-Guadalquivir-Doñana High (AGDH) corresponding to the seismic horizon *T1*. Three sectors of the AGDH are shown as differentiated based on different characteristics and faulting (GEFZ and F4). Green line: distal limit of the GCAW. Burgundy lines: active faults (Cabral et al., 2017 and references therein). Red lines: location of seismic sections where the AGDH appears. Abbreviations given in Fig. 3 caption. (For interpretation of the references to colour in this figure legend, the reader is referred to the web version of this article.)

sector 1 (<0.7 s TWT) relative to that observed in sector 3 (Figs. 5a, 7). In sector 2, the AGDH crops out locally along the seafloor at water depths of ~450 m. The AGDH represents the southern boundary of the Algarve Basin and marks a ~ NE-SW area of reduced *U3* thickness (0.04 s to 1.16 s TWT, Fig. 3c).

Diapiric structures

Several diapiric structures occur along the Algarve, Doñana, Sanlucar and Cadiz Basins (Fig. 3b, c). These structures appear as isolated bodies or elongated ridges such as the Guadalquivir and Cadiz Diapiric Ridges, which separate the Doñana, Sanlucar and Cadiz Basins.

Diapir-related deformation occurs more intensively in wedge-top basins, where features form a network that encases small depocentres (Fig. 3c). In seismic sections, the diapirs exhibit chaotic to transparent seismic facies intruding *U1* or *U2* and sometimes the lower *U3* (Figs. 4a, 5, 7a). The diapirs deform the upper sub-units of *U3* with small-scale faults developed on top of the diapir or by folding of the overburden (Figs. 4a, 5). Some of the diapirs occur in association with the tectonic structures described above. Within the Gil Eanes Fault zone, a diapiric structure intrudes the east-bounding fault F2, which extends for at least 15 km in a NE-SW orientation (Figs. 3b, c, 4a). The Cadiz Fault mimics the orientation of the Guadalquivir Diapiric Ridge and shows a diapiric structure developed along the fault for ~110 km (Figs. 3b, c, 5).

4.4. Seismicity analysis

A significant number of seismic events (>6000) have occurred in this region (Fig. 8; see Figs. S1 and S2). Events tend to exhibit low to intermediate magnitude (ML = 0.1 to 6.1) and occur at shallow (<5 km) to intermediate depths (<80 km). Most of the earthquakes occur at depths of 10–31 km with very few events below 40 km (Fig. S1). Event magnitudes tend to categorize as micro-seismic (ML < 1.9; Fig. S2). The focal mechanisms solutions in Fig. 8a (details in Table S2) show predominantly reverse fault motion (AGDH sector 3, Gil Eanes and Cadiz faults).

Earthquake clusters occurred along the AGDH in sectors 2 (in the ENE) and 3 covering the Algarve and Doñana Basins (Fig. 8a) with most hypocentres between 20 and 29 km depth. Few earthquakes seem to have occurred along the Cadiz Fault rendering it the boundary of a zone with intensive seismic activity (Fig. 8a). The focal mechanism solutions in Fig. 8a (details in Table S2) show predominantly reverse motion (AGDH sector 3, Gil Eanes and Cadiz faults). Several transpressional

events occurred along the AGDH sector 1 and the Cadiz Fault (codes 2, 6 and 10 in Fig. 8a and Table S2). A single normal event (code 1 in Fig. 8a and Table S2) occurred in AGDH sector 2 (the Guadalquivir Bank) at a depth of 32.9 km. In the northern Gil Eanes Fault Zone, seismicity occurred mostly between depths of 10 to 29 km and with magnitudes ML < 1.9 (Fig. 8a, Fig. S2). To the south of this feature, deeper events occurred (20–39 km and a few at >40 km depth) including one strike-slip event (code 9 in Fig. 8a and Table S2).

The P1 profile, a vertical cross-section that extends along the southern Gil Eanes Fault Zone (Fig. 8b), shows that most hypocentres display a complex distribution and occurred at depths between ~12 and 32 km. A second profile cutting across the Cadiz Fault (P2 in Fig. 8c) shows numerous, dispersed hypocentres along the NW side of the profile mostly at depths of 10–32 km. The SE of this profile and map shows fewer events (Fig. 8a). A sub-horizontal layer of hypocentres along the cross-sections P1 and P2 occurs at 32 km depth. Location estimates of these events are somewhat uncertain.

5. Discussion

5.1. Chronostratigraphic constraints

The basement of the study area consists of Palaeozoic rocks (Vázquez et al., 2015; Ramos et al., 2017) and appears only locally in the AGDH, where it is overlain by seismic horizon *T1* (Fig. 3a). Seismic unit *U1* correlates with folded Mesozoic (Triassic, Jurassic and Lower Cretaceous) and Palaeogene rocks (e.g., Ramos et al., 2017) of the inverted rifted margin.

Seismic horizon *T2* marks a basin-scale erosional episode separating *U1* from younger and less deformed sediments of seismic unit *U3* in the Algarve Basin (Fig. 3a). These relations indicate *T2* correlates with the basal foredeep unconformity (~8.2 Ma; Fig. 9) identified by Ledesma (2000) and Maldonado et al. (1999) in the Guadalquivir Basin. In the NW Algarve Basin, where the deformation associated to the Betic orogeny was less intense, it is preserved an older unconformity (~20.5 Ma) that roughly correlates with the seismic horizon *T2* (Roque et al., 2012). It is also recognised in the onshore part of the Algarve Basin, where it separates Upper Cretaceous from Middle Miocene deposits (Terrinha et al., 2019b). Thus, the unconformity is diachronous representing several tectonic events that affected the margin during the Miocene.

Seismic unit *U2* corresponds to the GCAW and consists of deformed Triassic, Cretaceous, Palaeogene and Neogene units (Maldonado et al., 1999). Seismic horizon *T3* corresponds to the top of the GCAW. Given its final emplacement around 8 Ma ago, it likely formed in the late Tortonian (Maldonado et al., 1999; Iribarren et al., 2007). This seismic horizon then underwent more deformation during the Pliocene and Quaternary.

Seismic unit *U3* spans a Neogene-Quaternary timeframe with the older deposits having a Burdigalian age in the NW Algarve Basin (Roque et al., 2012), but Tortonian above the GCAW (Ng et al., 2021a, 2021b), and the younger deposits corresponding to the Holocene (e.g., Llave et al., 2011; Roque et al., 2012; Hernández-Molina et al., 2016, Table 1 and Fig. 9).

Fig. 9 shows detailed ages for *U3* sub-units together with the main turbidite and contourite deposits that characterise this seismic unit. Seismic horizon *a* correlates with the intra-Messinian Unconformity (~6.4 Ma). This unconformity shows a regional change in sedimentation from predominantly contouritic to hemipelagic deposits at about 6.4 Ma, while turbiditic deposits still appear locally (Ng et al., 2021b). Age estimates for the seismic discontinuities *b* to *f* were based on correlating these horizons with discontinuities described by Hernández-Molina et al. (2016); Figs. 2, 9). The seismic horizon *b* corresponds to the Late Pliocene discontinuity (LPD, 3.2–3.0 Ma), and *c* corresponds to the Early Quaternary discontinuity (EQD, 2.3–2.0 Ma). Seismic horizon *d* correlates with a ~ 1.5–1.3 Ma discontinuity, and *e* correlates with the Middle
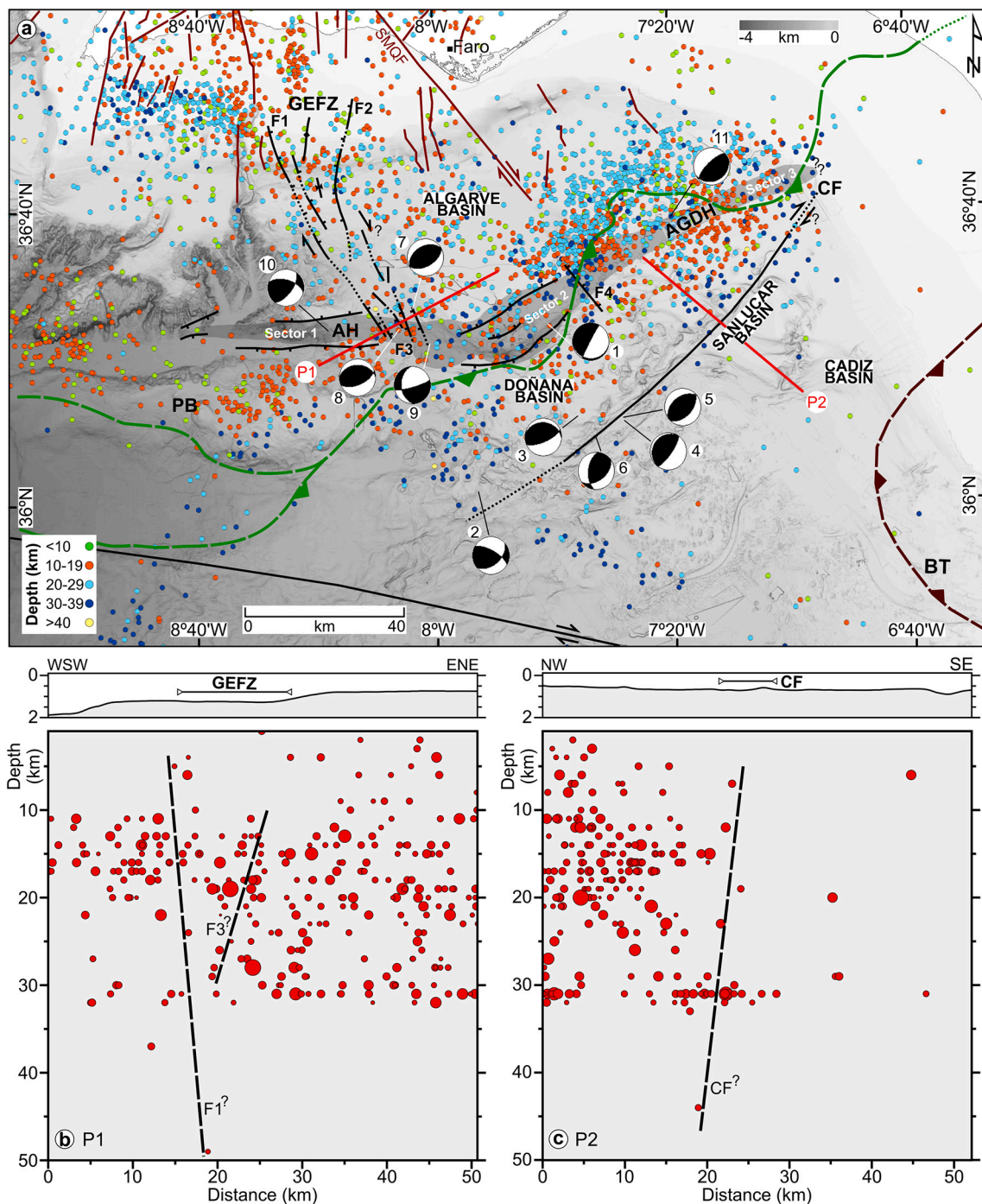
Fig. 8. Earthquake distribution in the study area. a) regional epicentres distribution map and the estimated focal mechanisms (codes 1–11; see Supplementary Material Fig. S1, S2 and Table S2 for further information). Burgundy lines: active faults (Cabral et al., 2017); b) Cross-section and bathymetric profile P1 across the GEFZ southern sector and c) cross-section and bathymetric profile P2 along the wedge-top sector across the CF. Bathymetric profiles have a vertical exaggeration of 5× and the earthquakes projected are located within a 40 km radius. Abbreviations given in Fig. 1 and Fig. 3 captions. (For interpretation of the references to colour in this figure legend, the reader is referred to the web version of this article.)

Pleistocene discontinuity (MPD, 0.9–0.7 Ma). Seismic horizon *f* corre- lates to the Late Quaternary discontinuity (LQD, 0.6–0.3 Ma).

5.2. Tectono-sedimentary domains

The character of seismic units, their regional structure and seismicity distribution suggested four tectonic-sedimentary domains (A, B, C and D in Fig. 10). These domains coincide roughly with the GCCS morphose- dimentary sectors proposed by Hernández-Molina et al. (2003, 2006)

and Llave et al. (2007).

Domain A

Domain A occurs in front of the Betic Orogen, which includes the Sanlucar and Cadiz Basins (northwest of BT in Fig. 10a). These basins developed on top of the GCAW (*U2*) and constitute the main depocentre (max. of 2.77 s TWT, Fig. 3c and Table S3) for the late Miocene- Quaternary deposits (*U3*, Fig. 10b). Poor seismic resolution precluded detection of *U3a* and the lower part of *U3b* (< 5.33 Ma) in these two
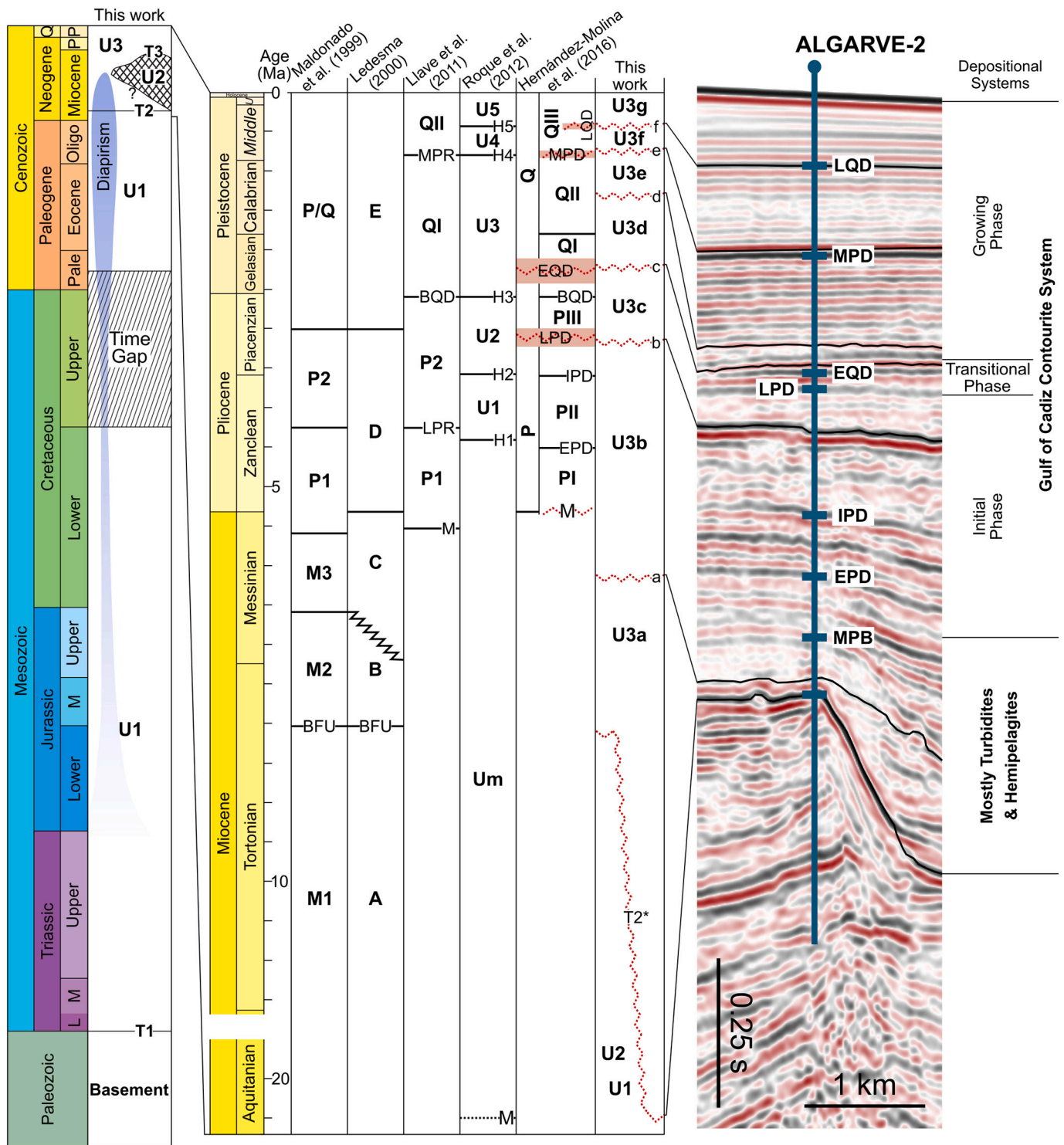
Fig. 9. Chronostratigraphic chart and correlation of *U3* tectonostratigraphic seismic sub-units with previously published seismostratigraphic models for the Miocene-Quaternary Algarve Basin. BFU: Basal Foredeep Unconformity, M: Miocene-Pliocene Boundary, EPD: Early Pliocene Discontinuity, IPD: Intra Pliocene Discontinuity, LPD: Late Pliocene Discontinuity, BQD: Base Quaternary Discontinuity, EQD: Early Quaternary Discontinuity, MPD: Middle Pleistocene Discontinuity and LQD: Late Quaternary Discontinuity. *Locally, the base of *U3a* is the seismic horizon *T1* (above the AGDH Sector 2) and *T3* (above the GCAW).

basins, but seismic facies and the geometry of the deposits can indicate that these sub-units consist primarily of hemipelagites and muddy contourites (Tables 1 and 2, Figs. 5a, 10b; Hernández-Molina et al., 2016; Ng et al., 2021a, 2021b). Upwards, in upper parts of *U3b* to *U3g*, along-slope deposits gradually become predominant and sheeted drifts appear (Figs. 9, 10b; e.g., Hernández-Molina et al., 2016). Nevertheless, evidence for local down-slope processes, such as erosional channels, also

appears throughout the seismic sequence (Fig. 10b). These channels seem to erode pre- or *syn*-depositional contourite deposits.

Diapirism is a major process influencing the northern part of this domain (Fig. 10a), where a network of diapiric structures controls depocentre distribution (Fig. 3c). Diapiric structures consist of a combination of Triassic evaporites and Miocene clays and marls (e.g., Fernández-Puga et al., 2007; Medialdea et al., 2009). Some of these
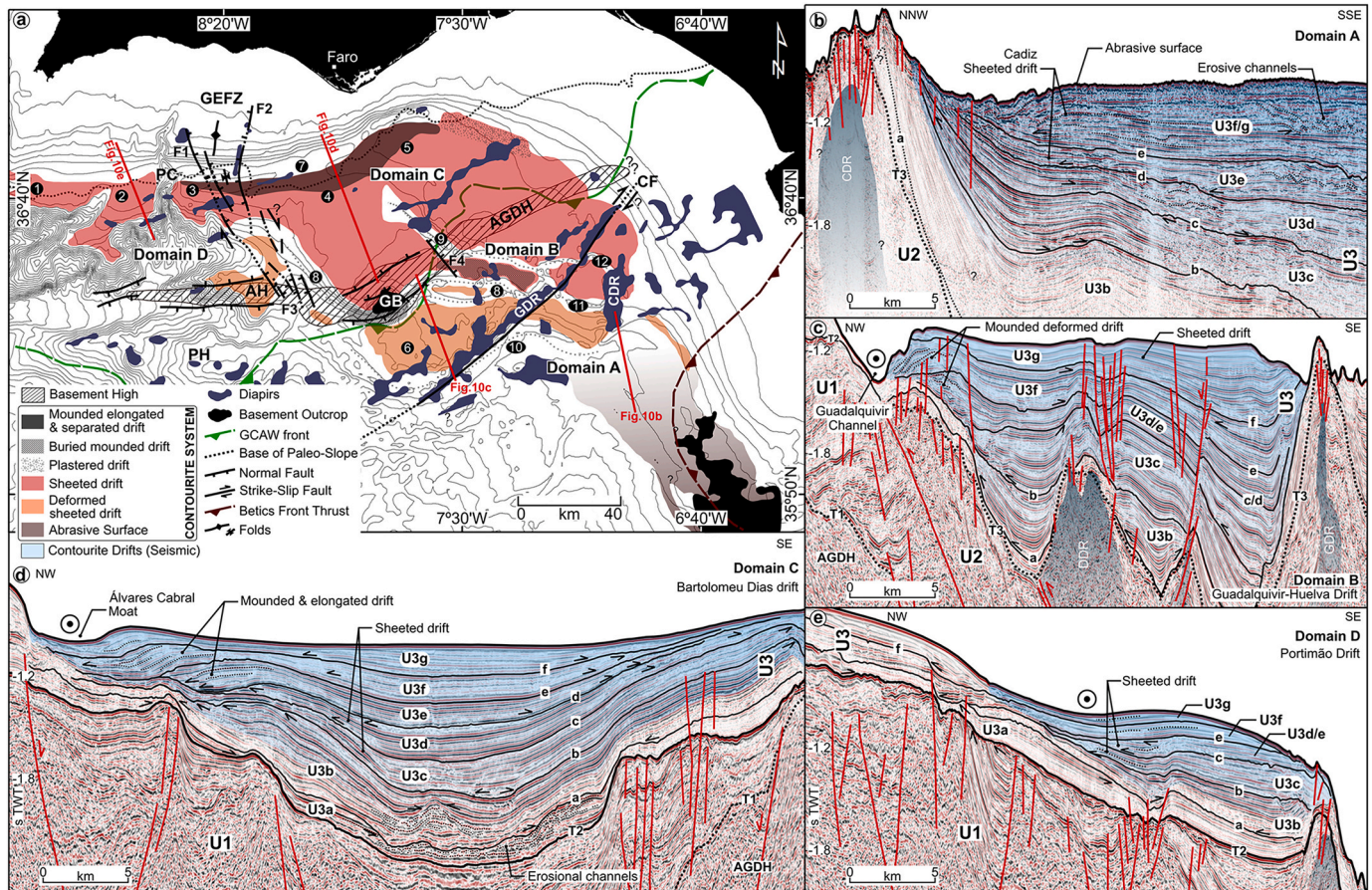
Fig. 10. Tectono-sedimentary domains identified in the Gulf of Cadiz (A, B, C and D) and their relations with the contourite depositional system. a) Map showing the four tectonic domains and the depositional and erosional features associated with the GCDS (adapted from Hernández-Molina et al., 2006): 1) Lagos drift, 2) Portimão drift, 3) Albufeira drift, 4) Bartolomeu Dias drift, 5) Faro drift, 6) Guadalquivir-Huelva drift, 7) Álvares Contourite Moat, 8) Guadalquivir channel, 9) Diogo Cão channel, 10) Cadiz channel and 11) Huelva channel. Panels b), c), d) and e) show seismic lines for the large contourite features in each of the tectonic domains. DDR: Doñana Diapiric Ridge, PC: Portimão Canyon. Abbreviations given in Fig. 3 caption.

diapirs (e.g., the Cadiz Diapiric Ridge, Fig. 10b) locally deform the present-day seafloor and create bathymetric highs that restrict lateral extension of drifts (Fig. 10b) and control MOW pathways (Fig. 10a). Diapiric activity may also influence turbiditic deposits observed in this domain wherein vertical growth of diapirs creates local instabilities in the sedimentary sequence. Most of Domain A exhibits a gentle seafloor without major variation in relief and only local diapiric deformation (see Fig. 10b). This favours the widening of the MOW circulation. Sheeted drifts observed in Domain A (Fig. 10b) formed as a consequence of the wider, non-focused current (Faugères and Stow, 2008; Roque et al., 2012). Presently, the surface consists of sand dunes and ribbons (proximal scour and sand-ribbons morphosedimentary sector, Hernández-Molina et al., 2006) suggesting current enhancement.

Seismic analysis indicates this domain corresponds to the almost aseismic zone observed S-SE of the Cadiz Fault (Fig. 8a, c). Given that the subduction in the Gibraltar Arc may have ceased in Miocene times, these observations support interpretations of a dormant accretionary wedge (Maldonado et al., 1999; Gràcia et al., 2003; Vergés and Fernàndez, 2012). However, seismicity and diapiric activity indicate ongoing regional deformation (Figs. 3b, c, 8a). Modern deformation of the GCAW also appears in seismic reflection and refraction data (Gutscher et al., 2002, 2009), in bathymetric data (Gutscher et al., 2009) and in analogue modelling experiments (Duarte et al., 2011).

Domain B

Domain B corresponds to the Doñana Basin, which is separated from Domain A by the Cadiz Fault (Fig. 10a). As with the previous domain,

late Miocene-Quaternary infill (*U3*; depocentres dW-6 and dW-7, Fig. 3c and Table S3) developed on top of the GCAW (*U2*). The basin consists primarily of contourite deposits with mounded drifts that evolve upwards into sheeted geometries (Fig. 6b, 10c; Llave et al., 2007).

This domain exhibits intensive diapirism, which controlled the sedimentary depocentre's evolution (Figs. 3c, 10a) by increasing accommodation space via downbuilding processes lateral to diapiric features. Diapiric structures similar to those observed as Domain A influenced the growth of drifts and show a shift in internal geometries from mounded to sheeted. Diapiric processes are also responsible for the observed internal deformation of the contourite deposits (Figs. 5b, 10c), which demonstrate syn- and post-depositional diapiric activity during the Late Miocene-Quaternary timeframe. In contrast to Domain A, diapirism within Domain B strongly affects the present-day seafloor morphology directly or by associated faulting and/or folding (Figs. 1b, 10c). Diapirism also causes deflection of the MOW current pathway and consequent formation of an intricate network of erosive channels (Fig. 10a; e.g., García et al., 2009; Hernández-Molina et al., 2003). This domain corresponds to the channels and ridges morphosedimentary sector (Fig. 1b), described by Hernández-Molina et al. (2006).

The present analysis could not determine whether the Cadiz Fault represents an inherited structure. The seismic data specifically do not resolve its relationship with syn-extensional strata (units below *U2*, Fig. 5). Despite this, the Cadiz Fault trends in an orientation consistent with the *E*-W to ENE-WSW rift normal faults (Terrinha et al., 2003, 2019a; Ramos et al., 2020). Although the seismic data did not offer clear kinematic indication, focal mechanisms associated with the Cadiz Fault

(Fig. 8a, Table S2) and regional tectonic setting (westward movement of the Betic-Rif orogenic system; e.g., Vergés and Fernàndez, 2012) suggest a dextral transpressional motion.

Domain B (Doñana Basin) hosted a high number of seismic events throughout (Fig. 8a). The transition between this seismic region and the aseismic Domain A occurs near the present-day GCAW front and in close association with the Cadiz Fault (Profile P2 in Fig. 8c). These spatial relations suggest that the front represents a lithospheric-scale structure and may be a remnant of earlier tectonic events.

Domain C

Domain C corresponds to the eastern Algarve Basin (Fig. 10a) and is separated from Domain B by the Albufeira-Guadalquivir-Doñana High (AGDH). Similar to the Cadiz Fault, this structure trends in orientations consistent with the normal faults developed during Mesozoic rifting (Terrinha et al., 2003, 2019a; Ramos et al., 2020). The structural high is bounded by several extensional faults (Fig. 6) and is thus interpreted as an inherited extensional horst. The AGDH Sector 2 exhibited normal faulting (code 1 in Fig. 8a and Table S2) at a depth of 32.9 km. The depth of this structure made it difficult to relate to potential reactivation of structural highs.

In this domain, the late Miocene-Quaternary sequence (*U3*) developed above the inverted margin (*U1*) in the elongated depression east of the Gil Eanes Fault Zone (dA-1 to dA-5, Fig. 3c and Table S3). *U3* consists of turbidite deposits and erosional channels (*U3a*) and prevalent contourite deposits (*U3b-U3g*), whose mounded drifts evolve basinward into sheeted geometries (Figs. 5b, c, 9, 10d; Llave et al., 2001; Hernández-Molina et al., 2006, 2016; Roque et al., 2012). The position of this domain as the submarine continuation of the Guadalquivir foreland basin indicates that Domain C also subsided during the late Miocene-Quaternary (Ledesma, 2000; Garcia-Castellanos et al., 2002; Salvany et al., 2011) due to tectonic loading by the Betic Orogen and changes in lithospheric mantle thickness (Garcia-Castellanos et al., 2002). Subsidence created accommodation space in the eastern Algarve Basin thereby favouring preferential accumulation of contourite drifts in this domain. The contourite deposits grew considerably in size (~50 km width and 75 km length) and thickness (max. ~1.75 s TWT) to become the main depositional sector of the GCCS (Fig. 10d). As noted above, this domain corresponds to the contourite-deposition morpho-sedimentary sector described by Hernández-Molina et al. (2003, 2006); Fig. 1b).

The regional seismicity map shows a high earthquake density in Domain C. Scattered seismicity occurs along the Algarve Basin and a cluster of events occurred NE of the Guadalquivir Bank in AGDH sectors 2 and 3 (Fig. 8a). Deformation in foreland basin systems typically migrates rapidly through the accretionary wedge towards the foreland (e. g., Apennines Orogeny, Ghielmi et al., 2013). The recent convergence between Nubia and Iberia seems to be accommodated near the GCAW front (the Doñana Basin region; Domain B) and the adjacent foredeep (Domain C). This interpretation offers a better explanation for the absence of seismic activity in the innermost region of the GCAW than hypotheses of accretionary wedge inactivity.

Domain D

On the western side of the Gil Eanes Fault (Fig. 10a), Domain D hosts only one small sedimentary depocentre (dA-6; Fig. 3b and Table S3). The rest of this zone consists of a thin *U3* (<1.35 s TWT). The NW-SE-oriented Gil Eanes Fault zone trends in a direction consistent with rift transfer zone structures such as the São Marcos-Quarteira Fault (Cabral et al., 2017, 2019; Fig. 1b). The negative flower-structure observed in seismic profiles (Fig. 4a, b, c) and the strike-slip focal mechanism of an event occurring at 32 km depth observed in the southern Gil Eanes Fault (code 10 in Fig. 8a and Table S2) support this interpretation, and thus we suggest a dextral movement for this structure. At high resolution, Profile P1 (Fig. 8b) shows sub-vertical lineaments of hypocentres in the region of this fault zone (F1 and F3, at 15–28 km; Fig. 8a, b) with a deep event occurring at ~49 km. The deeper events demonstrate that the Gil Eanes

Fault is a lithospheric-scale structure.

As in Domain C, the late Miocene-Quaternary infill (*U3*; part of dA-5 and dA-6, Fig. 3c) developed on top of the inverted margin (*U1*). It comprises hemipelagic and turbiditic deposits (*U3a* and lower *U3b*, Tables 1, 2 and Fig. 10e), and sheeted to mounded contourite drifts (upper *U3b* to *U3g*; Tables 1, 2 and Fig. 10e) (Hernández-Molina et al., 2016; Ng et al., 2021a, 2021b).

The limited development of U3 in the western Algarve region (Fig. 10e) suggests limited accommodation space or sedimentary input. Consistent with the lack of sedimentary depocentres (only dA-6, Fig. 3c), contourite drifts become less extensive in this domain where they span 10–15 km in width and ~ 50 km in length (Fig. 10e). A history of uplift rather than subsidence of Domain D may explain the lesser degree of accommodation space relative to Domain C. Onshore deposits show similar patterns. SW Portugal experiences higher rates of uplift (0.04 to 0.09 mm/yr) than the SE Algarve (0.03 mm/yr; Figueiredo, 2015; Neves et al., 2015). Pereira and Alves (2013) also suggested that the area between the S and SW Iberian margins where Domain D occurs corresponded to a major structural high separating the rift domains of the central North Atlantic and west Tethys during the Mesozoic. The narrow and incised slope morphology (Hernández-Molina et al., 2006; Fig. 1b) is clearly steeper (up to >20°) than that of other domains (<5°). This could contribute to the lack of depocentres in Domain D. Portimão Canyon (Fig. 10a) can also capture the MOW upper core (Marchès et al., 2007), which reduces its intensity and leads to smaller depositional features. Furthermore, Portimão and Lagos Canyons drain the shelf and upper slope sediments directly into the lower slope and thus limit sedimentary accumulation in the upper slope.

5.3. Tectono-sedimentary evolutionary stages

The late Miocene-Quaternary record of SW Iberia documents a complex interplay between sedimentary, palaeoceanographic and tectonic processes (e.g., Duggen et al., 2003; Medialdea et al., 2004; Terrinha et al., 2009; Zitellini et al., 2009; Duarte et al., 2013; Flecker et al., 2015; Hernández-Molina et al., 2016; Llave et al., 2011; Terrinha et al., 2019a, 2019b).

Three tectono-sedimentary evolution stages were identified since the late Miocene according to the major regional events that conditioned the margin and its deep-water sedimentary system. These regional events are: i) the Betic-Rif orogeny at ~8 Ma (e.g., Maldonado et al., 1999; Medialdea et al., 2004; Vergés and Fernàndez, 2012; Terrinha et al., 2019a, 2019b), ii) closing and re-opening of the Gibraltar Strait, due to vertical lithospheric movements (e.g., Duggen et al., 2003; Krijgsman et al., 2018) and iii) the latest reorganization of the Nubia-Iberia plates and onset of a transpressive tectonic regime at around 2.0–1.8 Ma (Rosas et al., 2009; Zitellini et al., 2009).

Stage 1 (8.0 Ma – 5.3 Ma)

The seismic unit *U1*, composed of Mesozoic and Paleogene-middle Miocene deposits, was deformed before the late Miocene (Terrinha et al., 2019b). The GCAW (*U2*) was emplaced in the Gulf of Cadiz during the in the last compressional phases of the Betic-Rif orogeny, which peak occurred in the late Tortonian at ~8 Ma (Vergés and Fernàndez, 2012). The lower part of unit *U3* (sub-units *U3a* and early *U3b*; ~8.0–5.33 Ma) was deposited above a major erosional unconformity (seismic horizon *T2*) that marks the beginning of the foredeep setting in the eastern Algarve Basin (DeCelles and Giles, 1996). Eastward, in the Doñana, Sanlucar and Cadiz basins it developed on top of the GCAW, burying the frontal part of the accretionary wedge. These basins formed as the wedge-top sector (DeCelles and Giles, 1996) of the foreland basin system'.

The morphology of the study area's seafloor between 8.0 and 5.3 Ma (Fig. 3b) differed markedly from that presently observed (Fig. 1). An ENE-WSW Algarve elongated depression (Domain C, probably continuing further SW into Domain D, Figs. 3b, 10a, d) likely formed a

wide submarine valley (depocentres dA-1, dA-2, dA-3 and dA-4 in Fig. 3c). It extended NE into the Spanish margin to join the onshore Guadalquivir Basin. By contrast, the Albufeira-Guadalquivir-Doñana High limited deposition of sub-units *U3a* and *U3b* as indicated by their minor thickness in this area (Figs. 5a, 7b). The structure appeared to play an important role in shaping basin architecture during the late Miocene by establishing the boundary between the foredeep and wedge-top depozones (Figs. 3c, 7). Another structure that played an important role was the Gil Eanes Fault, which influenced late Miocene sedimentation by creating local accommodation space along the extension of the fault zone where sub-units *U3a* and the lower part of *U3b* appear thicker (Fig. 4b, c). Throughout the late Miocene, the connection between the Atlantic Ocean and the Mediterranean Sea was established through the Betic and Rifian corridors and possibly also through Gibraltar (Flecker et al., 2015; Krijgsman et al., 2018). This suggests that the Algarve valley (Domain C) represents the western continuation of the Betic Atlantic-Mediterranean gateway, through which the palaeo-MOW circulated. In the wedge-top sector, the palaeo-morphology documents widespread diapiric intrusions (Fig. 3b), but Domains A and B indicate a similar drainage direction. Incision of turbidite channels as observed in the upper parts of sub-unit *U3a* along the Algarve valley axis (Fig. 3b, Tables 1 and 2) suggests the predominance of down-slope processes in the early Messinian (<6.4 Ma). The same turbiditic system appears in the Guadalquivir Basin, along the Cadiz continental shelf (Riaza and Del Olmo, 1996; Ledesma, 2000) and in the Rharb Basin (Capella et al., 2017). Local contourite features also appear (Martín et al., 2009; Capella et al., 2017; de Weger et al., 2020; Ng et al., 2021b) in association with paleo-MOW circulation prior to the Messinian Salinity Crisis. Vertical lithospheric movements closed the gateways (Duggen et al., 2003). The Betic corridor closed around 7.2 Ma and the Rifian corridor at 6.8 Ma to trigger the Messinian Salinity Crisis (5.97–5.33 Ma; Flecker et al., 2015). A regional middle to upper Messinian hemipelagic unit (~6.4–5.33 Ma) overlies the turbidite and contourite deposits across the margin (Ng et al., 2021b). Seismic horizon *a* (~6.4 Ma) documents this change in sedimentation and indicates a decrease in tectonic activity in the Gulf of Cadiz region.

Stage 2 (5.3 Ma – 2.0 Ma)

The Messinian Salinity Crisis ended at 5.33 Ma (Miocene-Pliocene boundary) with the re-opening of the Strait of Gibraltar (Duggen et al., 2003; Flecker et al., 2015; Krijgsman et al., 2018). This event changed the oceanographic circulation in the Gulf of Cadiz by allowing the MOW to flow into the Atlantic Ocean. The onset of widespread contourite deposition in the Gulf of Cadiz area ensued (Llave et al., 2001; Roque et al., 2012; Hernández-Molina et al., 2016). Sub-unit *U3b* deposited during early stages of weak MOW circulation and represents the GCCS' initial phase of drift deposition (5.33–3.2 Ma, Fig. 9; Hernández-Molina et al., 2014a, 2014b). The unit exhibits a mixture of contourites with intercalated turbidites and debrites (Hernández-Molina et al., 2016). Sub-unit *U3c* deposited during the subsequent transitional drift phase (3.2–2.0 Ma, Fig. 9), which consisted of up-slope drift migration and moat development (Hernández-Molina et al., 2016). The change in drift configuration suggests enhancement of bottom current circulation coinciding with shifting climatic conditions from humid to cold and arid in the late Pliocene at 3.4 Ma (Béthoux and Pierre, 1999). The MOW became saltier, cooler and denser leading to current intensification along the Iberian margin (Khélifi et al., 2009; Hernández-Molina et al., 2014a, 2014b; Hernández-Molina et al., 2016). Seismic horizon *b* (Fig. 9) records the shift in drift morphology and lithology (sub-units *U3b* to *U3c*), which corresponds to a compressional phase at about 3.2–3.0 Ma. The age of this horizon indicates that it is contemporaneous to a shift in the Iberia-Nubia plate boundary from N-S to NNW-SSE that occurred at this time (Maldonado et al., 1999). The subsidence episode observed in the Algarve Basin, which hosts extensive contourite deposits (Domain C, Fig. 10d), also offers evidence of tectonic activity prior to the LPD discontinuity (seismic horizon *b*).

The change in sedimentation associated with seismic horizon *b* may also relate to a decrease in tectonic activity after the hiatus associated with the LPD. In this case, turbidites and debris deposits reflect slope failure and instability caused by tectonic activity (Teixeira et al., 2019) with contourite deposition becoming dominant under more stable conditions. The Gil Eanes Fault zone continued to influence the basins by separating the uplifted sector of the margin (Domain D) from the Algarve Basin foredeep (Fig. 10b, e), while providing accommodation space through movement along its trace (similar that operating in Miocene times; Fig. 4). The fault's role diminishes with time with *U3c* only showing thickness variation south of the fault zone (Fig. 4c). This suggests that the Gil Eanes Fault becomes less active or even inactive in accordance with a previously hypothesized decrease in tectonic activity (at about 3.0 Ma). The AGDH continues to influence sediment distribution during the Pliocene. The upper part of *U3b* and *U3c* still exhibit reduced thicknesses on top of the structural high (Figs. 5a, 6b). This feature also acted locally to separate the MOW into different branches (Figs. 1, 10a; García et al., 2009) and thereby form different contourite drifts in the Algarve (Bartolomeu Dias drift in Domain C, Figs. 6b, 10a) and Doñana Basins (Guadalquivir-Huelva drift in domain B, Figs. 6b, 10a). Diapirism also influences depocentres of the Doñana, Sanlucar and Cadiz Basins (as can be seen in Fig. 3c) as evident from sediment distribution (Figs. 5, 10a, b, c).

Stage 3 (2 Ma – 0 Ma)

Final Iberia-Nubia plate boundary reorganization during the Gelasian resulted in a regional shift from a NW-SE transpressive regime to one of WNW–ESE compression (Terrinha et al., 2009; Zitellini et al., 2009; Cunha et al., 2012). Rosas et al. (2009) interpreted analogue models and quantitative strain markers indicating SWIM faults reactivated as strike-slip features by 1.8 Ma. However, Hernández-Molina et al. (2016) correlated this event with the Early Quaternary Discontinuity (EQD, 2.3–2.0 Ma) found within GCCS contourite deposits. Seismic horizon *c* marks this subsidence episode in the eastern Algarve Basin (Domain C; Fig. 10d). This horizon corresponds to a regional unconformity in the tectono-sedimentary Domains A, B and D (Figs. 4a, 10b, c, d, e) for the given time frame.

According to Hernández-Molina et al. (2014a, 2014b); Hernández-Molina et al., 2016), sub-units *U3d* to *U3g* formed during the growth-drift phase of the GCCS (Fig. 9), which began at about 2 Ma, coeval with a strengthening of MOW circulation. Contourite deposits appear as mounded and elongated drifts with moats in the Algarve Basin (Table 2, Fig. 10d) and sandier sheeted drifts in the wedge-top basins (Table 2, Fig. 10b, c). The consistent sedimentary staking patterns exhibited by contourite deposits suggest stable persistence of depositional conditions during this time. Diapiric activity also influenced depocentre distribution and local deformation of sub-units *U3d* to *U3g* in Domains A and B (Figs. 5, 10c). The network of diapiric structures acted to separate local depocentres and thereby determined accommodation space for sub-units (Fig. 3c).

Drifts recognised in Domains C and D continue to exhibit distinct characteristics (e.g., dimension) related to the different histories of these domains (Fig. 10d, e). Subsidence in Domain C intensified during this period (after seismic horizon *d*, 1.5–1.3 Ma?) as recorded by seismic sub-units *U3e*, *U3f* and *U3g*. Seismic horizons *e* (MPD 0.9–0.7 Ma) and *f* (LQD 0.6–0.3 Ma), which separated the aforementioned sub-units, correlated with phases of MOW intensification identified by Hernández-Molina et al. (2016). These occurred after the 1.3–1.0 Ma glacial MOW period. Interpretations usually attribute bottom current enhancement to global climatic and sea-level changes, but tectonic control cannot be excluded.

Previous research has documented evidence of Quaternary deformation in the Gulf of Cadiz region (Gràcia et al., 2003; Rosas et al., 2009; Crutchley et al., 2011; Custódio et al., 2015; Silva et al., 2017; Cabral et al., 2019; Luján et al., 2020; Silva et al., 2020). Reactivation of WNW-ESE SWIM faults as strike-slip structures since 1.8 Ma offers compelling evidence of this deformation (Rosas et al., 2009). In onshore regions of

the Algarve region, recent activity of the São Marcos-Quarteira Fault deformed sediments deposited between 1.8 Ma and 130 ka (Cabral et al., 2019). Present-day tectonic processes continue to influence the study area as demonstrated by the extensive seismicity recorded (Fig. 8a, Custódio et al., 2015; Silva et al., 2017). The predominance of reverse focal mechanism solutions (Fig. 8a, Table S2) indicates continuing compression along the margin. This demonstrates the role of tectonic mechanisms in the on-going development of contourite features and seafloor morphology (see details in 5.4).

5.4. Structural controls on contourite system evolution

Tectonic processes directly and indirectly control the evolution of sedimentary basins at regional and local scales by influencing their sedimentary architecture and depositional processes. The GCCS exhibits different depositional and erosional features in each of the tectonic domains described above (Fig. 10a). Three types of structural control have been identified as the main elements involved in the development of the GCCS. These are i) tectonic vertical movements, such as subsidence or uplift, ii) fault-related depressions and iii) the presence of structural obstacles (Fig. 11).

Tectonic vertical movements

Tectonic vertical movements are widely known as being responsible for shaping the regional topography and by creation or destruction of accommodation space at a broad scale. Thus, besides changes in the bottom-current strength related to climate and eustatic variations, the size and thickness of contourite deposits also reflects the space available for sediment accumulation (Fig. 11a). In fact, despite being formed by the influence of the MOW upper core flowing along the SW Iberian Slope (Fig. 1b), contourite deposits developed in these tectono-sedimentary domains show different characteristics (Fig. 10a, d, e) due to contrasts in the inherited configuration of the Algarve Basin (Fig. 11a). In the study area, it is observed that the main depositional sector of the contourite system and where the deposits are thicker and wider (Fig. 3c,

Table S3) occurs in Domain C where subsidence was recognised (Bartolomeu Dias Drift, Fig. 10a, d). Due to several Pliocene and Quaternary subsidence episodes (details in 5.3), this area permitted the creation of accommodation space and favours the development of these depocentres (Fig. 3c). Contrarily, in domains having experienced regional uplift as Domain D (Fig. 10a), the observed contourite drift deposits (Portimão Drift, Fig. 10e) were less extensive (Fig. 3c, Table S3). The uplift affecting Domain D enhances erosional processes by increasingly elevating the seafloor relief, leading to the steepening the slope and causing instabilities. It also reduces accommodation space and consequently sediment accumulation. If a region is characterised by bathymetric lows or undergoes subsidence, the space for drift deposition is increased when compared with areas undergoing uplift. Researchers have described similar contourite deposit patterns in response to variations in tectonically controlled depositional space for the Hikurangi subduction margin of New Zealand (Bailey et al., 2021) and in other deep-water environments (Clark and Cartwright, 2009; Leeder, 2011).

Tectonic structures

Tectonic structures such as fault zones, basement highs and diapirs can also condition the accumulation and geometry of contourite deposits, as they locally affect the seafloor morphology by creating negative or positive reliefs (Fig. 11b, c). Their impact on contourites can be direct, by creating accommodation space locally for sediment deposition or indirect by influencing bottom-currents circulation pathways and strength. The Guadalquivir and Diogo Cão contourite channels developed in a NW-SE orientation along the southern Gil Eanes Fault Zone and F4 faults, respectively (Figs. 4c, 10a). This suggests the influence of these faults in the development of some sectors of the contourite channels (e.g., circulation through the local depressions resulting from the faults' negative flower structures). The depressed areas associated with negative flower structures act as a favourable path for bottom-current circulation confining and enhancing the flow, favouring the erosion of the seafloor (Figs. 4, 11b). García et al. (2016) previously suggested structural control of the Diogo Cão contourite channel by the São
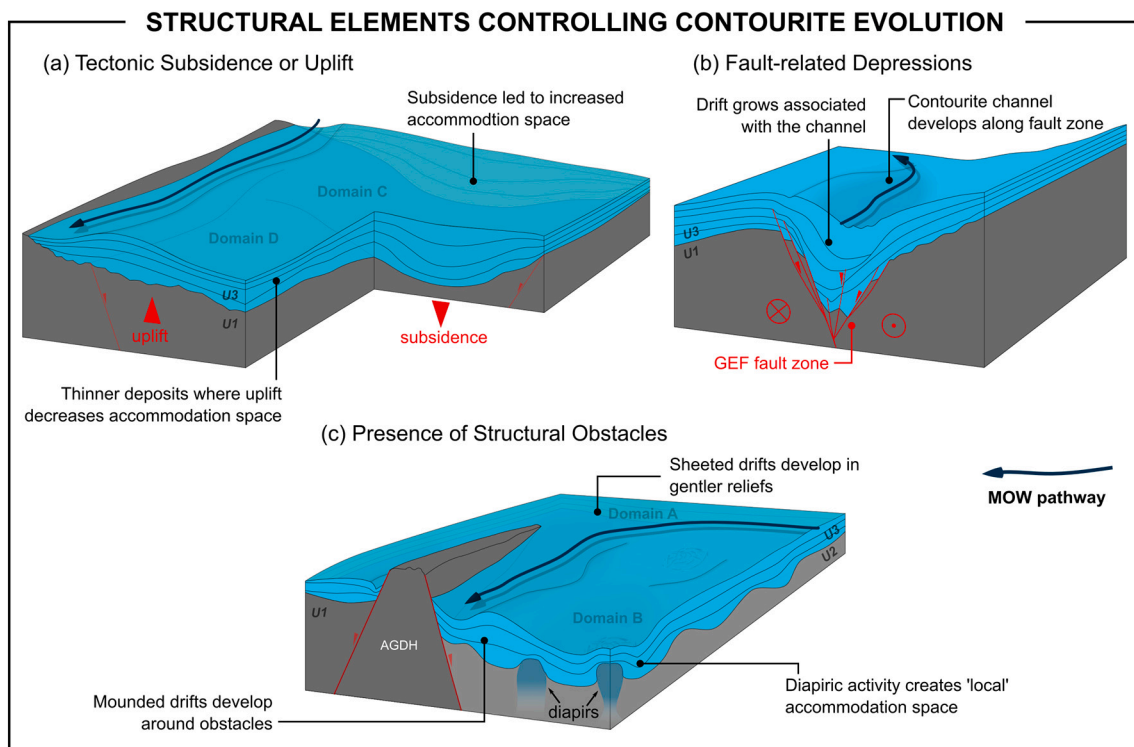
Fig. 11. 3D sketches showing the structural elements controlling contourite evolution including tectonic subsidence or uplift (a), the presence of structural obstacles (b) and fault-related depressions (c). Not to scale.

Marcos-Quarteira Fault. The identification of F4 and the Gil Eanes Fault in the present study demonstrates the importance of inherited margin structures in development of the GCCS. Previous research has recognised the interaction between fault-related depressions and channel distribution in other types of deep-water deposits and specifically the confinement or diversion of turbidite channels in the Levante Basin of the eastern Mediterranean (Clark and Cartwright, 2009, 2011). In the southern Gil Eanes Fault Zone, a contourite drift was recognised extending through the Guadalquivir channel (Figs. 4c, 10a). We suggest that this feature formed due to the combination of the confinement of the MOW discussed above and the local increase of accommodation space in this area. This is another evidence of fault-related morphology controlling deposition of the GCCS.

Local subsidence induced by diapiric processes also was an important influence on the evolution of contourite deposits in the study area. Diapiric activity has a strong influence on the northern part of Domain A and Domain B (Fig. 10a, b, c), with a network of diapiric structures controlling sediment distribution and restrict the lateral extension of the deposits (Fig. 10b). Depocentre formation occur laterally to areas of diapir rise, increasing accommodation space due to downbuilding processes. The available space for sediment accumulation is variable over time, being directly related to the intensity of diapiric activity, but also influenced by sediment input and current strength driven by climate and eustatic changes.

The presence of structural obstacles on the seafloor, such as structural highs and fault-scarps, can lead to changes of bottom-currents pathways and strength. In the Northern Hemisphere, due to the Coriolis Effect, the currents are diverted to the right, as is seen by the MOW behaviour after it crosses the Strait of Gibraltar and enters the Gulf of Cadiz (Fig. 1b). If any structural feature creates an important increase of the seafloor slope gradients and is oriented perpendicularly to the direction of flow, the current is forced to diverge from its path contouring the obstacle (Fig. 11c). In the study area, this can be observed along the AGDH and diapiric structures with seafloor expression (e.g., Guadalquivir Diapiric Ridge; Figs. 1b, 6b, 10) in the tectono-sedimentary domains A and B (Fig. 10a). Accordingly, the type of contourite drifts developed is a consequence of the interaction of the MOW with seafloor reliefs, which causes local enhancement of flow velocity along the foot of the reliefs (Faugères and Stow, 2008). The focusing of the MOW circulation around these features increases the erosion along the foot of the obstacles (forming contourite moats or channels) and favours the lateral deposition of drifts with mounded and separated geometries, as seen in Domain B (Figs. 10c, 11c). By contrast, when the seafloor consists of smooth and gentle relief, such as in Domain A (Fig. 10b), the bottom-current flow tends to be laminate and therefore the resulting contourite deposits exhibit a sheeted geometry (Fig. 11c). These drift shapes' related to slower bottom-current circulation conditions (Faugères and Stow, 2008), prevail when the MOW can flow more uniformly along the SW Iberian Margin middle slope as in the case of the Bartolomeu Dias Drift (Fig. 10d). Therefore, tectonic structures have a direct impact in bottom-current circulation pathway and strength, which consequently controls the type of deposit that is formed. Thus strong, focused currents lead to mounded drifts, while weaker currents are usually associated with smooth seafloors and can lead to the development of sheeted drifts. The type of contourite drift (i.e., sheeted, mounded and separated) may thus reflect basin-scale palaeo-topography and structural features, besides the characteristic of the bottom-currents and its changes through time. Similar variations in contourite drift geometries due to the presence of structural positive reliefs have been reported for the SW Adriatic margin (Pellegrini et al., 2016), the southern Bay of Biscay (Liu et al., 2019) and the South China Sea (Liu et al., 2021).

Although, the different types of contourite deposits the Gulf of Cadiz have generally been correlated to MOW changes driven by shorter term global climate and eustatic sea-level fluctuations (e.g., Faugères and Stow, 2008; Hernández-Molina et al., 2006, 2016), the tectonic processes and resulting structures also played a significant role as a long term first-order control on contourite drift accumulation.

6. Conclusions

This study evaluated relations between tectonic history and depositional features in the Gulf of Cadiz. It identified two major structural boundaries in the study area. The newly identified Gil Eanes Fault bounds the western terminus of the Algarve foredeep basin. The Cadiz Fault divides the margin into different lithospheric segments. Palaeobathymetric relief inherited from the rifted continental margin influences the structural style of the Algarve, Doñana, Sanlucar and Cadiz basins. These inherited structures determine margin configuration and delineate physiographic domains. They also determine late Miocene sedimentary evolution including the main depositional and erosional features of the Gulf of Cadiz Contourite Depositional System.

The sedimentary stacking pattern and bathymetry of the study area reflect the interaction of regional tectonic processes, which conditioned seafloor irregularities, and diapiric activity. Three main tectonostratigraphic stages have been recognised in the Gulf of Cadiz evolution: at 8–5.3 Ma; 5.3–2.0 Ma and from 2.0 Ma to present day. Tectonic activity during these stages specifically controlled the position, dimension and types of the contourite depositional features through time. The size and geometry of contourite drifts depend on tectonically controlled depositional space at basin scale. Structural positive reliefs such as the AGDH and diapirs can influence contourite drift morphologies, because their steep and usually abrupt slopes forced the current to contour them and thus favouring the accumulation of mounded and separated contourite drifts. The associated moat develops close to the relief' slope by enhancement of flow velocity along the foot of these structural highs. By contrast, when the seafloor I characterised by smooth and gentle relief, the bottom-current circulation is slower and the contourite deposits exhibit sheeted geometries.

These results of this study demonstrate the salient role of margin structure and tectonics in the development of contourite depositional systems. They control the sea-floor relief and in turn in influenced the local oceanic circulation processes that determining the morphology and sedimentary evolution of contourite systems. The study can serve as a reference for future research on deep-water systems in active settings or areas with complex inherited bathymetry (e.g., the Brazilian margin, the Bahamas and the Mozambique Channel).

Data availability statement

Supporting data for this study were provided by TGS and REPSOL under confidentiality agreements. The restrictions do not allow open sharing of the proprietary data used in this research, but data are available upon reasonable request made to the authors and with permissions from TGS and REPSOL.

Declaration of Competing Interest

The authors declare that they have no known competing financial interests or personal relationships that could have appeared to influence the work reported in this paper.

Appendix A. Supplementary data

Supplementary data to this article can be found online at https://doi.org/10.1016/j.margeo.2022.106818.

References

Ambar, I., Howe, M.R., 1979. Observations of the mediterranean outflow - II the deep circulation in the vicinity of the Gulf of Cadiz. Deep Sea Res. Part A Oceanogr. Res. Pap. 26, 555–568. https://doi.org/10.1016/0198-0149(79)90096-7.

Artoni, A., Rizzini, F., Roveri, M., Gennari, R., Manzi, V., Papani, G., Bernini, M., 2007. Tectonic and climatic controls on sedimentation in late Miocene Cortemaggiore Wedge-Top Basin (Northwestern Apennines, Italy). In: Lacombe, O., Lavé, J., Roure, F., Vergés, J. (Eds.), Thrust Belts and Foreland Basins: From Fold Kinematics to Hydrocarbon Systems. Springer, Berlin, pp. 431–456.

Bailey, W.S., McArthur, A.D., McCaffrey, W.D., 2021. Distribution of contourite drifts on convergent margins: examples from the Hikurangi subduction margin of New Zealand. Sedimentology 294–323. https://doi.org/10.1111/sed.12779.

Baptista, M.A., Miranda, P.M.A., Miranda, J.M., Mendes Victor, L., 1998. Constrains on the source of the 1755 Lisbon tsunami inferred from numerical modelling of historical data on the source of the 1755 Lisbon tsunami. J. Geodyn. 25, 159–174. https://doi.org/10.1016/S0264-3707(97)00020-3.

Béthoux, J.-P., Pierre, C., 1999. Mediterranean functioning and sapropel formation: respective influences of climate and hydrological changes in the Atlantic and the Mediterranean. Mar. Geol. 153, 29–39. https://doi.org/10.1016/S0025-3227(98)00091-7.

Cabral, J., Mendes, V.B., Figueiredo, P., da Silveira, A.B., Pagarete, J., Ribeiro, A., Dias, R., Ressurreição, R., 2017. Active tectonics in Southern Portugal (SW Iberia) inferred from GPS data. Implications on the regional geodynamics. J. Geodyn. 112, 1–11. https://doi.org/10.1016/j.jog.2017.10.002.

Cabral, J., Dias, R.P., Cunha, P.P., Cabral, M.C., 2019. Quaternary tectonic activity of the São Marcos–Quarteira fault (Algarve, southern Portugal): a case study for the characterization of the active geodynamic setting of SW Iberia. J. Iber. Geol. 1–16 https://doi.org/10.1007/s41513-019-00102-2.

Capella, W., Hernández-Molina, F.J., Flecker, R., Hilgen, F.J., Hssain, M., Kouwenhoven, T.J., van Oorschot, M., Sierro, F.J., Stow, D.A.V., Trabucho-Alexandre, J., Tulbure, M.A., de Weger, W., Yousfi, M.Z., Krijgsman, W., 2017. Sandy contourite drift in the late Miocene Rifian Corridor (Morocco): Reconstruction of depositional environments in a foreland-basin seaway. Sediment. Geol. 355, 31–57. https://doi.org/10.1016/j.sedgeo.2017.04.004.

Capella, W., Barhoun, N., Flecker, R., Hilgen, F.J., Kouwenhoven, T., Matenco, L.C., Sierro, F.J., Tulbure, M.A., Yousfi, M.Z., Krijgsman, W., 2018. Palaeogeographic evolution of the late Miocene Rifian Corridor (Morocco): reconstructions from surface and subsurface data. Earth-Science Rev. 180, 37–59. https://doi.org/10.1016/j.earscirev.2018.02.017.

Carlini, A., Chelli, A., Vescovi, P., Artoni, A., Clemenzi, L., Tellini, C., Torelli, L., 2016. Tectonic control on the development and distribution of large landslides in the Northern Apennines (Italy). Geomorphology 253, 425–437. https://doi.org/10.1016/j.geomorph.2015.10.028.

Clark, I.R., Cartwright, J.A., 2009. Interactions between submarine channel systems and deformation in Deepwater fold belts: examples from the Levant Basin, Eastern Mediterranean Sea. Mar. Pet. Geol. 26, 1465–1482. https://doi.org/10.1016/j.marpetgeo.2009.05.004.

Clark, I.R., Cartwright, J.A., 2011. Key controls on submarine channel development in structurally active settings. Mar. Pet. Geol. 28, 1333–1349. https://doi.org/10.1016/j.marpetgeo.2011.02.001.

Crutchley, G.J., Berndt, C., Klaeschen, D., Masson, D.G., 2011. Insights into active deformation in the Gulf of Cadiz from new 3-D seismic and high-resolution bathymetry data. Geochemistry Geophys. Geosystems 12, 1–20. https://doi.org/10.1029/2011GC003576.

Cunha, T.A., Matias, L.M., Terrinha, P., Negredo, A.M., Rosas, F., Fernandes, R.M.S., Pinheiro, L.M., 2012. Neotectonics of the SW Iberia margin, Gulf of Cadiz and Alboran Sea: a reassessment including recent structural, seismic and geodetic data. Geophys. J. Int. 188, 850–872. https://doi.org/10.1111/j.1365-246X.2011.05328.x.

Custódio, S., Dias, N.A., Carrilho, F., Góngora, E., Rio, I., Marreiros, C., Morais, I., Alves, P., Matias, L., 2015. Earthquakes in western Iberia: improving the understanding of lithospheric deformation in a slowly deforming region. Geophys. J. Int. 203, 127–145. https://doi.org/10.1093/gji/ggv285.

de Weger, W., Hernández-Molina, F.J., Flecker, R., Sierro, F.J., Chiarella, D., Krijgsman, W., Manar, M.A., 2020. Late Miocene contourite channel system reveals

intermittent overflow behavior. Geology 48, 1194–1199. https://doi.org/10.1130/g47944.1.

de Weger, W., Hernández-Molina, F.J., Miguez-Salas, O., de Castro, S., Bruno, M., Chiarella, D., Sierro, F.J., Blackbourn, G., Manar, M.A., 2021. Contourite depositional system after the exit of a strait: case study from the late miocene South Rifian corridor, Morocco. Sedimentology. https://doi.org/10.1111/sed.12882.

DeCelles, P.G., Giles, K.A., 1996. Foreland basin systems. Basin Res. 8, 105–123. https://doi.org/10.1046/j.1365-2117.1996.01491.x.

Duarte, J.C., Rosas, F.M., Terrinha, P., Gutscher, M.A., Malavieille, J., Silva, S., Matias, L., 2011. Thrust wrench interference tectonics in the Gulf of Cadiz (Africa-Iberia plate boundary in the North-East Atlantic): Insights from analog models. Mar. Geol. 289, 135–149. https://doi.org/10.1016/j.margeo.2011.09.014.

Duarte, J.C., Rosas, F.M., Terrinha, P., Schellart, W.P., Boutelier, D., Gutscher, M.A., Ribeiro, A., 2013. Are subduction zones invading the Atlantic? Evidence from the Southwest Iberia margin. Geology 41, 839–842. https://doi.org/10.1130/G34100.1.

Duggen, S., Hoernle, K., van den Bogaard, Paul, Rüpke, L., Phipps Morgan, J., Ru, L., Morgan, J.P., Duggen, S., Van Den Bogaard, P., Rüpke, L., van den Bogaard, Paul, 2003. Deep roots of the Messinian salinity crisis. Nature 422, 602–606, 10.1038/nature01553.

EMODnet Bathymetry Consortium, 2018. EMODnet Digital Bathymetry (DTM 2018) [WWW Document]. https://doi.org/10.12770/18ff0d48-b203-4a65-94a9-5fd8b0ec35f6.

Faugères, J.C., Stow, D.A.V., 2008. Contourite drifts. Nature, evolution and controls. In: Rebesco, M., Camerlenghi, A. (Eds.), Contourites, Developments in Sedimentology, volume 60. Elsevier, pp. 259–288. https://doi.org/10.1016/S0070-4571(08)10014-0.

Fernández-Puga, M.C., Vázquez, J.T., Somoza, L., Díaz del Río, V., Medialdea, T., Mata, M.P., León, R., 2007. Gas-related morphologies and diapirism in the Gulf of Cádiz. Geo-Marine Lett. 27, 213–221. https://doi.org/10.1007/s00367-007-0076-0.

Figueiredo, P.C. dos S., 2015. Neotectonics of the Southwest Portugal Mainland: Implications on the Regional Seismic Hazard (doctoral dissertation). University of Lisbon, Lisboa, Portugal.

Flecker, R., Krijgsman, W., Capella, W., de Castro Martíns, C., Dmitrieva, E., Mayser, J.P., Marzocchi, A., Modestu, S., Ochoa, D., Simon, D., Tulbure, M., van den Berg, B., van der Schee, M., de Lange, G., Ellam, R., Govers, R., Gutjahr, M., Hilgen, F., Kouwenhoven, T., Lofi, J., Meijer, P., Sierro, F.J., Bachiri, N., Barhoun, N., Alami, A. C., Chacon, B., Flores, J.A., Gregory, J., Howard, J., Lunt, D., Ochoa, M., Pancost, R., Vincent, S., Yousfi, M.Z., 2015. Evolution of the late Miocene Mediterranean-Atlantic gateways and their impact on regional and global environmental change. Earth-Science Rev. 150, 365–392. https://doi.org/10.1016/j.earscirev.2015.08.007.

Fukao, Y., 1973. Thrust faulting at a Lithospheric plate boundary, the Portugal earthquake of 1969. Earth an 18 (2), 205–216. https://doi.org/10.1016/0012-821X(73)90058-7.

García, M., Hernández-Molina, F.J., Llave, E., Stow, D.A.V., León, R., Fernández-Puga, M. C., Diaz del Río, V., Somoza, L., 2009. Contourite erosive features caused by the Mediterranean Outflow Water in the Gulf of Cadiz: Quaternary tectonic and oceanographic implications. Mar. Geol. 257, 24–40. https://doi.org/10.1016/j.margeo.2008.10.009.

García, M., Hernández-Molina, F.J., Alonso, B., Vázquez, J.T., Ercilla, G., Llave, E., Casas, D., 2016. Erosive sub-circular depressions on the Guadalquivir Bank (Gulf of Cadiz): Interaction between bottom current, mass-wasting and tectonic processes. Mar. Geol. 378, 5–19. https://doi.org/10.1016/j.margeo.2015.10.004.

García, M., Llave, E., Hernández-Molina, F.J., Lobo, F.J., Ercilla, G., Alonso, B., Casas, D., Mena, A., Fernández-Salas, L.M., 2020. The role of late Quaternary tectonic activity and sea-level changes on sedimentary processes interaction in the Gulf of Cadiz upper and middle continental slope (SW Iberia). Mar. Pet. Geol. 121, 104595 https://doi.org/10.1016/j.marpetgeo.2020.104595.

Garcia-Castellanos, D., Fernández, M., Torne, M., 2002. Modeling the evolution of the Guadalquivir foreland basin (southern Spain). Tectonics 21. https://doi.org/10.1029/2001TC001339, 9-1-9–17.

Geissler, W.H., Matias, L., Stich, D., Carrilho, F., Jokat, W., Monna, S., IbenBrahim, A., Mancilla, F., Gutscher, M.-A., Sallarès, V., Zitellini, N., 2010. Focal mechanisms for sub-crustal earthquakes in the Gulf of Cadiz from a dense OBS deployment. Geophys. Res. Lett. 37, L18309. https://doi.org/10.1029/2010GL044289.

Ghielmi, M., Minervini, M., Nini, C., Rogledi, S., Rossi, M., 2013. Late Miocene-Middle Pleistocene sequences in the Po Plain - Northern Adriatic Sea (Italy): the stratigraphic record of modification phases affecting a complex foreland basin. Mar. Pet. Geol. 42, 50–81. https://doi.org/10.1016/j.marpetgeo.2012.11.007.

Gràcia, E., Dañobeitia, J., Vergés, J., Bartolomé, R., Córdoba, D., 2003. Crustal architecture and tectonic evolution of the Gulf of Cadiz (SW Iberian margin) at the convergence of the Eurasian and African plates. Tectonics 22 (4). https://doi.org/10.1029/2001TC901045.

Grevemeyer, I., Matias, L., Silva, S., 2016. Mantle earthquakes beneath the South Iberia continental margin and Gulf of Cadiz – constraints from an onshore-offshore seismological network. J. Geodyn. 99, 39–50. https://doi.org/10.1016/j.jog.2016.06.001.

Gutscher, M.-A., Malod, J., Rehault, J.-P., Contrucci, I., Klingelhoefer, F., Mendes-Victor, L., Spakman, W., 2002. Evidence for active subduction beneath Gibraltar. Geology 30 (12), 1071–1074. https://doi.org/10.1130/0091-7613(2002)030<1071:EFASBG>2.0.CO;2.

Gutscher, M.A., Dominguez, S., Westbrook, G.K., Gente, P., Babonneau, N., Mulder, T., Gonthier, E., Bartolome, R., Luis, J., Rosas, F., Terrinha, P., 2009. Tectonic shortening and gravitational spreading in the Gulf of Cadiz accretionary wedge: Observations from multi-beam bathymetry and seismic profiling. Mar. Pet. Geol. 26, 647–659. https://doi.org/10.1016/j.marpetgeo.2007.11.008.

Hernández-Molina, J., Llave, E., Somoza, L., Fernández-Puga, M.C., Maestro, A., León, R., Medialdea, T., Barnolas, A., García, M., Díaz del Río, V., Fernández-Salas, L.M., Vázquez, J.T., Lobo, F., Alveirinho Dias, J.M., Rodero, J., Gardner, J., 2003. Looking for clues to paleoceanographic imprints: a diagnosis of the Gulf of Cadiz contourite depositional systems. Geology 31, 19–22. https://doi.org/10.1130/0091-7613 (2003)031<0019:LFCTPI>2.0.CO;2.

Hernández-Molina, F.J., Llave, E., Stow, D.A.V., García, M., Somoza, L., Vázquez, J.T., Lobo, F.J., Maestro, A., Díaz del Río, V., León, R., Medialdea, T., Gardner, J., 2006. The contourite depositional system of the Gulf of Cádiz: a sedimentary model related to the bottom current activity of the Mediterranean outflow water and its interaction with the continental margin. Deep. Res. Part II Top Stud. Oceanogr. 53, 1420–1463. https://doi.org/10.1016/j.dsr2.2006.04.016.

Hernández-Molina, F.J., Llave, E., Preu, B., Ercilla, G., Fontan, A., Bruno, M., Serra, N., Gomiz, J.J., Brackenridge, R.E., Sierro, F.J., Stow, D.A.V., García, M., Juan, C., Sandoval, N., Arnaiz, A., 2014a. Contourite processes associated with the Mediterranean Outflow Water after its exit from the Strait of Gibraltar: Global and conceptual implications. Geology 42, 227–230. https://doi.org/10.1130/G35083.1.

Hernández-Molina, F.J., Stow, D.A.V., Alvarez-Zarikian, C.A., Acton, G., Bahr, A., Balestra, B., Ducassou, E., Flood, R., Flores, J.-A., Furota, S., Grunert, P., Hodell, D., Jimenez-Espejo, F., Kim, J.K., Krissek, L., Roque, C., Pereira, H., Fernanda, M., Goñi, S., Sierro, F.J., Singh, A.D., Sloss, C., Takashimizu, Y., Tzanova, A., Voelker, A., Williams, T., Xuan, C., 2014b. Onset of Mediterranean outflow into the North Atlantic. Science 344, 1244–1250. https://doi.org/10.1126/science.1251306.

Hernández-Molina, F.J., Sierro, F.J., Llave, E., Roque, C., Stow, D.A.V., Williams, T., Lofi, J., Van der Schee, M., Arnáiz, A., Ledesma, S., Rosales, C., Rodríguez-Tovar, F.J., Pardo-Igúzquiza, E., Brackenridge, R.E., 2016. Evolution of the gulf of Cadiz margin and Southwest Portugal contourite depositional system: tectonic, sedimentary and paleoceanographic implications from IODP expedition 339. Mar. Geol. 377, 7–39. https://doi.org/10.1016/j.margeo.2015.09.013.

Iribarren, L., Vergés, J., Camurri, F., Fullea, J., Fernàndez, M., 2007. The structure of the Atlantic-Mediterranean transition zone from the Alboran Sea to the Horseshoe Abyssal Plain (Iberia-Africa plate boundary). Mar. Geol. 243, 97–119. https://doi.org/10.1016/j.margeo.2007.05.011.

Iribarren, L., Vergés, J., Fernàndez, M., 2009. Sediment supply from the Betic–Rif orogen to basins through Neogene. Tectonophysics 475 (1), 68–84. https://doi.org/10.1016/j.tecto.2008.11.029.

Johnston, A.C., 1996. Seismic moment assessment of earthquakes in stable continental regions – III. New Madrid 1811-1812, Charleston 1886 and Lisbon 1755. Geophys. J. Int. 126, 314–344. https://doi.org/10.1111/j.1365-246X.1996.tb06015.x.

Khélifi, N., Samthein, M., Andersen, N., Blanz, T., Frank, M., Garbe-Schönberg, D., Haley, B.A., Stumpf, R., Weinelt, M., 2009. A major and long-term Pliocene intensification of the Mediterranean outflow, 3.5-3.3 Ma ago. Geology 37, 811–814. https://doi.org/10.1130/G30058A.1.

Krijgsman, W., Capella, W., Simon, D., Hilgen, F.J., Kouwenhoven, T.J., Meijer, P.T., Sierro, F.J., Tulbure, M.A., van den Berg, Bas C.J., van der Schee, M., Flecker, R., van der Berg, B.C.J., van der Schee, M., Flecker, R., 2018. The Gibraltar corridor: watergate of the Messinian salinity crisis. Mar. Geol. 403, 238–246. https://doi.org/10.1016/j.margeo.2018.06.008.

Ledesma, S., 2000. Astrobiocronología y estratigrafía de alta resolución del neógeno de la cuenca del Guadalquivir-Golfo de Cádiz. PhD Thesis. Universidad de Salamanca, Salamanca.

Leeder, M.R., 2011. Tectonic sedimentology: Sediment systems deciphering global to local tectonics. Sedimentology 58, 2–56. https://doi.org/10.1111/j.1365-3091.2010.01207.x.

León, R., Urgeles, R., Pérez-López, R., Payo, E., Vázquez-Isquierdo, A., Giménez-Moreno, C.J., Casas, D., 2020. Geological and tectonic controls on morphometrics of submarine landslides of the Spanish margins. Geol. Soc. London Spec. Publ. 500, 495–513. https://doi.org/10.1144/SP500-2019-153.

Liu, S., Van Rooij, D.V., Vandorpe, T., González-Pola, C., Ercilla, G., Hernández-Molina, F.J., 2019. Morphological features and associated bottom-current dynamics in the LeDanois Bank region (southern Bay of Biscay, NE Atlantic): a model in atopographically constrained small basin. Deep-Sea Research Part I, 149. https://doi.org/10.1016/j.dsr.2019.05.014.

Liu, S., Hernández-Molina, F.J., Lei, Z., Duarte, D., Chen, H., Wang, C., Lei, Y., Zhuo, H., Huang, S., Zhang, L., Su, M., 2021. Fault-controlled contourite drifts in the southern South China Sea: Tectonic, oceanographic, and conceptual implications. Mar. Geol. 433 https://doi.org/10.1016/j.margeo.2021.106420.

Llave, E., Hernández-Molina, F.J., Somoza, L., Díaz del Río, V., Stow, D.A.V., Maestro, A., Alveirinho Dias, J.M., 2001. Seismic stacking pattern of the Faro-Albufeira contourite system (Gulf of Cadiz): a Quaternary record of paleoceanographic and tectonic influences. Mar. Geophys. Res. 22, 487–508. https://doi.org/10.1023/A:1016355801344.

Llave, E., Schönfeld, J., Hernández-Molina, F.J., Mulder, T., Somoza, L., Díaz Del Río, V., Sánchez-Almazo, I., 2006. High-resolution stratigraphy of the Mediterranean outflow contourite system in the Gulf of Cadiz during the late Pleistocene: the impact of Heinrich events. Mar. Geol. 227, 241–262. https://doi.org/10.1016/j.margeo.2005.11.015.

Llave, E., Hernández-Molina, F.J., Stow, D.A.V., Fernández-Puga, M.C., García, M., Vázquez, J.T., Maestro, A., Somoza, L., Díaz del Río, V., 2007. Reconstructions of the Mediterranean Outflow Water during the Quaternary based on the study of changes in buried mounded drift stacking pattern in the Gulf of Cadiz. Mar. Geophys. Res. 28, 379–394. https://doi.org/10.1007/s11001-007-9040-7.

Llave, E., Matias, H., Hernández-Molina, F.J., Ercilla, G., Stow, D.A.V., Medialdea, T., 2011. Pliocene-Quaternary contourites along the northern Gulf of Cadiz margin: Sedimentary stacking pattern and regional distribution. Geo-Marine Lett. 31, 377–390. https://doi.org/10.1007/s00367-011-0241-3.

Llave, E., Hernández-Molina, F.J., García, M., Ercilla, G., Roque, C., Juan, C., Mena, A., Preu, B., Van Rooij, D., Rebesco, M., Brackenridge, R., Jané, G., Gómez-ballesteros, M., Stow, D., 2019. Contourites along the Iberian continental margins: conceptual and economic implications. Geol. Soc. London Spec. Publ. 476, 403–436.

Luján, M., Lobo, F.J., Mestdagh, T., Vázquez, J.T., Fernández-Puga, M.C., van Rooij, D., 2020. Pliocene-quaternary deformational structures in the Eastern Algarve Continental Shelf, Gulf of Cadiz. Geogaceta 67, 3–6.

Mack, G.H., 1978. Tectonic control of sedimentation. In: Middleton, G.V., Church, M.J., Coniglio, M., Hardie, L.A., Longstaffe, F.J. (Eds.), Encyclopedia of Sediments and Sedimentary Rocks. Encyclopedia of Earth Sciences Series. Springer. https://doi.org/10.1007/978-1-4020-3609-5.

Maldonado, A., Somoza, L., Pallarés, L., 1999. The Betic orogen and the Iberian-African boundary in the Gulf of Cadiz: Geological evolution (Central North Atlantic). Mar. Geol. 155, 9–43. https://doi.org/10.1016/S0025-3227(98)00139-X.

Marchès, E., Mulder, T., Cremer, M., Bonnel, C., Hanquiez, V., Gonthier, E., Lecroart, P., 2007. Contourite drift construction influenced by capture of Mediterranean Outflow Water deep-sea current by the Portimão submarine canyon (Gulf of Cadiz, South Portugal). Mar. Geol. 242, 247–260. https://doi.org/10.1016/j.margeo.2007.03.013.

Martín, J.M., Braga, J.C., Aguirre, J., Puga-Bernabéu, Á., 2009. History and evolution of the North-Betic Strait (Prebetic Zone, Betic Cordillera): a narrow, early Tortonian, tidal-dominated, Atlantic-Mediterranean marine passage. Sediment. Geol. 216, 80–90. https://doi.org/10.1016/j.sedgeo.2009.01.005.

Matias, H., Kress, P., Terrinha, P., Mohriak, W., Menezes, P.T.L., Matias, L., Santos, F., Sandnes, F., 2011. Salt tectonics in the Western Gulf of Cadiz, Southwest Iberia. Am. Assoc. Pet. Geol. Bull. 95, 1667–1698. https://doi.org/10.1306/01271110032.

Medialdea, T., Vegas, R., Somoza, L., Vázquez, J.T., Maldonado, A., Díaz-Del-Río, V., Maestro, A., Córdoba, D., Fernández-Puga, M.C., 2004. Structure and evolution of the "Olistostrome" complex of the Gibraltar Arc in the Gulf of Cádiz (eastern Central Atlantic): evidence from two long seismic cross sections. Mar. Geol. 209, 173–198. https://doi.org/10.1016/j.margeo.2004.05.029.

Medialdea, T., Somoza, L., Pinheiro, L.M., Fernández-Puga, M.C., Vázquez, J.T., León, R., Ivanov, M.K., Magalhaes, V., Díaz-del-Río, V., Vegas, R., 2009. Tectonics and mud volcano development in the Gulf of Cádiz. Mar. Geol. 261, 48–63. https://doi.org/10.1016/j.margeo.2008.10.007.

Mestdagh, T., Lobo, F.J., Llave, E., Hernández-Molina, F.J., Ledesma, A.G., Puga-Bernabéu, Á., Fernández-Salas, L.-M., Van Rooij, D., 2020. Late Quaternary multi-genetic processes and products on the northern Gulf of Cadiz upper continental slope (SW Iberian Peninsula). Mar. Geol. 427, 106214 https://doi.org/10.1016/j.margeo.2020.106214.

Mitchum, R.M., Vail, P.R., Sangree, J.B., 1977a. Seismic stratigraphy and global changes of sea level, part 6: Stratigraphic interpretation of seismic reflection patterns in depositional sequences. In: Payton, C.E. (Ed.), Seismic Stratigraphy-Applications to Hydrocarbon Exploration. American Association of Petroleum Geologists, pp. 117–133.

Mitchum, R.M., Vail, P.R., Thompson III, S., 1977b. Seismic stratigraphy and global changes of sea level, part 2: The depositional sequence as a basic unit for stratigraphic analysis. In: Payton, C.E. (Ed.), Seismic Stratigraphy-Applications to Hydrocarbon Exploration. American Association of Petroleum Geologists, pp. 53–62.

Mitchum, R.M., Vail, P.R., Thompson III, S., 1977c. Seismic stratigraphy and global changes of sea level, part 1: Overview. In: Payton, C.E. (Ed.), Seismic Stratigraphy-Applications to Hydrocarbon Exploration. American Association of Petroleum Geologists, pp. 51–52.

Nelson, C.H., Baraza, J., Maldonado, A., Rodero, J., Escutia, C., Barber, J.H., 1999. Influence of the Atlantic inflow and Mediterranean outflow currents on late Quaternary sedimentary facies of the Gulf of Cadiz continental margin. Mar. Geol. 155, 99–129. https://doi.org/10.1016/S0025-3227(98)00143-1.

Neves, M.C., Figueiredo, P.M., Martínez-Loriente, S., 2015. Southwest Iberia uplift investigated by Flexural Modelling. Abstracts of the VIII Symposium on the Iberian Atlantic Margin.

Ng, Z.L., Hernández-Molina, F.J., Duarte, D., Roque, C., Sierro, F.J., Llave, E., Manar, M., 2021a. Late miocene contourite depositional system of the Gulf of Cadiz: the sedimentary signature of the paleo-Mediterranean Outflow Water. Mar. Geol. 442 https://doi.org/10.1016/j.margeo.2021.106605.

Ng, Z.L., Hernández-Molina, F.J., Duarte, D., Sierro, F.J., Ledesma, S.M., Rogerson, M., Llave, E., Roque, C., Manar, M.A., 2021b. Latest Miocene restriction of the Mediterranean Outflow Water: a perspective from the Gulf of Cádiz. Geo-Marine Lett. 41 https://doi.org/10.1007/s00367-021-00693-9.

Nikishin, A.M., Kopaevich, L.F., 2009. Tectonostratigraphy as a basis for paleotectonic reconstructions. Mosc. Univ. Geol. Bull. 64, 65–74. https://doi.org/10.3103/s014587520902001x.

Pereira, R., Alves, T.M., 2013. Crustal deformation and submarine canyon incision in a Meso-Cenozoic first order transfer zone (SW Iberia, North Atlantic Ocean). Tectonophysics 601, 148–162. https://doi.org/10.1016/j.tecto.2013.05.007.

Ramos, A., Fernández, O., Terrinha, P., Muñoz, J.A., 2016. Extension and inversion structures in the Tethys–Atlantic linkage zone, Algarve Basin. Portugal. Int. J. Earth Sci. 105, 1663–1679. https://doi.org/10.1007/s00531-015-1280-1.

Ramos, A., Fernández, O., Terrinha, P., Muñoz, J.A., 2017. Neogene to recent contraction and basin inversion along the Nubia-Iberia boundary in SW Iberia. Tectonics 36, 257–286. https://doi.org/10.1002/2016TC004262.

Ramos, A., Fernández, O., Terrinha, P., Muñoz, J.A., Arnaiz, Á., 2020. Paleogeographic evolution of a segmented oblique passive margin: the case of the SW Iberian margin. Int. J. Earth Sci. https://doi.org/10.1007/s00531-020-01878-w.

Riaza, C., Del Olmo, W.M., 1996. Depositional model of the Guadalquivir – Gulf of Cádiz Tertiary basin. In: Friend, P.F., Dabrio, C.J. (Eds.), Tertiary Basins of Spain: The

Stratigraphic Record of Crustal Kinematics, pp. 330–338. https://doi.org/10.1017/cbo9780511524851.047.

Rogerson, M., Rohling, E.J., Weaver, P.P.E., Murray, J.W., 2005. Glacial to interglacial changes in the settling depth of the Mediterranean Outflow plume. Paleoceanography 20, 1–12. https://doi.org/10.1029/2004PA001106.

Rogerson, M., Rohling, E.J., Bigg, G.R., Ramirez, J., 2012. Paleoceanography of the Atlantic-Mediterranean exchange: overview and first quantitative assessment of climatic forcing. Rev. Geophys. 50 https://doi.org/10.1029/2011RG000376.

Roque, C., Duarte, H., Terrinha, P., Valadares, V., Noiva, J., Cachão, M., Ferreira, J., Legoinha, P., Zitellini, N., 2012. Pliocene and Quaternary depositional model of the Algarve margin contourite drifts (Gulf of Cadiz, SW Iberia): Seismic architecture, tectonic control and paleoceanographic insights. Mar. Geol. 303–306, 42–62. https://doi.org/10.1016/j.margeo.2011.11.001.

Rosas, F.M., Duarte, J.C., Terrinha, P., Valadares, V., Matias, L., 2009. Morphotectonic characterization of major bathymetric lineaments in Gulf of Cadiz (Africa-Iberia plate boundary): Insights from analogue modelling experiments. Mar. Geol. 261, 33–47. https://doi.org/10.1016/j.margeo.2008.08.002.

Salvany, J.M., Larrasoañañ, J.C., Mediavilla, C., Rebollo, A., 2011. Chronology and tectono-sedimentary evolution of the Upper Pliocene to Quaternary deposits of the lower Guadalquivir foreland basin, SW Spain. Sediment. Geol. 241, 22–39. https://doi.org/10.1016/j.sedgeo.2011.09.009.

Sánchez-Leal, R.F., Bellanco, M.J., Fernández-Salas, L.M., García-Lafuente, J., Gasser-Rubinat, M., González-Pola, C., Hernández-Molina, F.J., Pelegrí, J.L., Peliz, A., Relvas, P., Roque, D., Ruiz-Villarreal, M., Sammartino, S., Sánchez-Garrido, J.C., 2017. The Mediterranean overflow in the Gulf of Cadiz: a rugged journey. Sci. Adv. 3, 1–12. https://doi.org/10.1126/sciadv.aao0609.

Serra, N., Ambar, I., Käse, R.H., 2005. Observations and numerical modelling of the Mediterranean outflow splitting and eddy generation. Deep Sea Res Part II Top. Stud. Oceanogr. 52, 383–408. https://doi.org/10.1016/j.dsr2.2004.05.025.

Sierro, F.J., Hodell, D.A., Andersen, N., Azibeiro, L.A., Jimenez-Espejo, F.J., Bahr, A., Flores, J.A., Ausin, B., Rogerson, M., Lozano-Luz, R., Lebreiro, S.M., Hernández-Molina, F.J., 2020. Mediterranean Overflow over the last 250 kyr: Freshwater Forcing from the Tropics to the Ice Sheets. Paleoceanogr. Paleoclimatology 35 (9). https://doi.org/10.1029/2020PA003931.

Silva, S., Terrinha, P., Matias, L., Duarte, J.C., Roque, C., Ranero, C.R., Geissler, W.H., Zitellini, N., 2017. Micro-seismicity in the Gulf of Cadiz: is there a link between micro-seismicity, high magnitude earthquakes and active faults? Tectonophysics 717, 226–241. https://doi.org/10.1016/j.tecto.2017.07.026.

Silva, P.F., Roque, C., Drago, T., Belén, A., Henry, B., Gemma, E., Lopes, A., López-González, N., Casas, D., Naughton, F., Vázquez, J.T., 2020. Multidisciplinary characterization of Quaternary mass movement deposits in the Portimão Bank (Gulf of Cadiz, SW Iberia). Mar. Geol. 420, 106086 https://doi.org/10.1016/j.margeo.2019.106086.

Spakman, W., Chertova, M.V., Van Den Berg, A., Van Hinsbergen, D.J.J., 2018. Puzzling features of western Mediterranean tectonics explained by slab dragging. Nat. Geosci. 11, 211–216. https://doi.org/10.1038/s41561-018-0066-z.

Stich, D., de Mancilla, F.L., Pondrelli, S., Morales, J., 2007. Source analysis of the February 12th 2007, Mw 6.0 Horseshoe earthquake: implications for the 1755 Lisbon earthquake. Geophys. Res. Lett. 34 https://doi.org/10.1029/2007GL030012.

Teixeira, M., Terrinha, P., Roque, C., Rosa, M., Ercilla, G., Casas, D., 2019. Interaction of alongslope and downslope processes in the Alentejo margin (SW Iberia) – Implications on slope stability. Mar. Geol. 410, 88–108. https://doi.org/10.1016/j.margeo.2018.12.011.

Terrinha, P., González-Clavijo, E.J., Vicente, J., Moniz, C., Dias, R., Vazquez, J.T., Diaz Del Rio, V., 2003. Falha de Portimão: novos dados, sobre a sua geometria e cinemática no Mesozóico, Neogénico e Quaternário e continuidade das estruturas nas áreas emersa e imersa do Algarve. Ciências da Terra special number V, pp. 101–105.

Terrinha, P., Matias, L., Vicente, J., Duarte, J., Luís, J., Pinheiro, L., Lourenço, N., Diez, S., Rosas, F., Magalhães, V., Valadares, V., Zitellini, N., Roque, C., Víctor, L.M.,

2009. Morphotectonics and strain partitioning at the Iberia-Africa plate boundary from multibeam and seismic reflection data. Mar. Geol. 267, 156–174. https://doi.org/10.1016/j.margeo.2009.09.012.

Terrinha, P., Rocha, R.B., Rey, J., Cachão, M., Moura, D., Roque, C., Martins, L., Valadares, V., Cabral, J., Azevedo, M.R., Barbero, L., Clavijo, E., Dias, R.P., Matias, H., Madeira, J., Silva, C.M., Munhá, J., Rebelo, L., Ribeiro, C., Vicente, J., Noiva, J., Youbi, N., Bensalah, M.K., 2013. A Bacia do Algarve: Estratigrafia, Paleogeografia e Tectónica. In: Dias, R., Araújo, A., Terrinha, P., Kullberg, J.C. (Eds.), Geologia de Portugal. Vol. II: Geologia Meso-Cenozóica de Portugal. Escolar Editora, Lisboa.

Terrinha, P., Kullberg, J.C., Neres, M., Alves, T., Ramos, A., Ribeiro, C., Mata, J., Pinheiro, L., Afilhado, A., Matias, L., Luís, J., Muñoz, J.A., 2019a. Rifting of the Southwest and West Iberia continental margins. In: Quesada, C., Oliveira, J.T. (Eds.), The Geology of Iberia: A Geodynamic Approach. Springer International Publishing, pp. 251–283. https://doi.org/10.1007/978-3-030-11295-0.

Terrinha, P., Ramos, A., Neres, M., Valadares, V., Duarte, J., Martínez-Loriente, S., Silva, S., Mata, J., Kullberg, J.C., Casas-Sainz, A., Matias, L., Fernández, Ó., Muñoz, J.A., Ribeiro, C., Font, E., Neves, C., Roque, C., Rosas, F., Pinheiro, L., Bartolomé, R., Sallarès, V., Magalhães, V., Medialdea, T., Somoza, L., Gràcia, E., Hensen, C., Gutscher, M.-A., Ribeiro, A., Zitellini, N., 2019b. The Alpine Orogeny in the West and Southwest Iberia margins. In: Quesada, C., Oliveira, J.T. (Eds.), The Geology of Iberia: A Geodynamic Approach. Springer International Publishing, Switzerland, pp. 487–505. https://doi.org/10.1007/978-3-030-11295-0.

Tilley, H., Moore, G.F., Underwood, M.B., Hernández-Molina, F.J., Yamashita, M., Kodaira, S., Nakanishi, A., 2021. Heterogeneous Sediment Input at the Nankai Trough Subduction Zone: implications for Shallow Slow Earthquake Location. Geochem. Geophys. Geosyst. 22 https://doi.org/10.1029/2021GC009965 e2021GC009965.

Tinterri, R., Tagliaferri, A., 2015. The syntectonic evolution of foredeep turbidites related to basin segmentation: Facies response to the increase in tectonic confinement (Marnoso-arenacea Formation, Miocene, Northern Apennines, Italy). Mar. Pet. Geol. 67, 81–110. https://doi.org/10.1016/j.marpetgeo.2015.04.006.

Vázquez, J.T., Alonso, B., Fernandez-Puga, M.C., Iglesias, J., Palomino, D., Roque, C., Ercilla, G., Diaz-del-Rio, V., Vazquez, J.-T., Alonso, B., Fernández-Puga, M.C., Gómez Ballesteros, M., Iglesias, J., Palomino, D., Roque, C., Ercilla, G., Díaz-del-Río, V., 2015. Seamounts along the Iberian continental margins. Bol. Geol. Min. 126, 483–514.

Vergés, J., Fernàndez, M., 2012. Tethys-Atlantic interaction along the Iberia-Africa plate boundary: the Betic-Rif orogenic system. Tectonophysics 579, 144–172. https://doi.org/10.1016/j.tecto.2012.08.032.

Voelker, A.H.L., Lebreiro, S.M., Schönfeld, J., Cacho, I., Erlenkeuser, H., Abrantes, F., 2006. Mediterranean outflow strengthening during northern hemisphere coolings: a salt source for the glacial Atlantic? Earth Planet. Sci. Lett. 245, 39–55. https://doi.org/10.1016/j.epsl.2006.03.014.

Watson, S.J., Mountjoy, J.J., Crutchley, G., 2020. Tectonic and geomorphic controls on the distribution of submarine landslides across active and passive margins, eastern New Zealand. Geol. Soc. London Spec. Publ. 500, 477–494. https://doi.org/10.1144/SP500-2019-165.

Wessel, P., Smith, W.H.F., 1998. New, improved version of generic mapping tools released. EOS Trans. Am. Geophys. Union 79, 579. https://doi.org/10.1029/98EO00426.

Zenk, W., Armi, L., 1990. The complex spreading pattern of Mediterranean Water off the Portuguese continental slope. Deep Sea Res. Part A Oceanogr. Res. Pap. 37, 1805–1823. https://doi.org/10.1016/0198-0149(90)90079-B.

Zitellini, N., Gràcia, E., Matias, L., Terrinha, P., Abreu, M.A., De Alteriis, G., Henriet, J.P., Dañobeitia, J.J., Masson, D.G., Mulder, T., Ramella, R., Somoza, L., Diez, S., 2009. The quest for the Africa-Eurasia plate boundary west of the Strait of Gibraltar. Earth Planet. Sci. Lett. 280, 13–50. https://doi.org/10.1016/j.epsl.2008.12.005.